HHS Public Access

Author manuscript

Cell Rep. Author manuscript; available in PMC 2020 June 14.

Published in final edited form as:

Cell Rep. 2020 April 14; 31(2): 107519. doi:10.1016/j.celrep.2020.03.083.

A Localized Scaffold for cGMP Increase Is Required for Apical Dendrite Development

Joanna Szczurkowska[1,8], **Seong-Il Lee**[1,8], **Alan Guo**[1], **Andrzej W. Cwetsch**[4,5], **Tanvir Khan**[1], **Sneha Rao**[1], **Gerd Walz**[2], **Tobias B. Huber**[3], **Laura Cancedda**[4,6], **Sophie Pautot**[7], **Maya Shelly**[1,9,*]

[1]Department of Neurobiology and Behavior, Stony Brook University, Stony Brook, NY 11794-5230, USA

[2]Department of Medicine IV, University Medical Center Freiburg, Faculty of Medicine, University of Freiburg, Freiburg im Breisgau, Germany

[3]III. Department of Medicine, University Medical Center Hamburg-Eppendorf, Hamburg, Germany

[4]Local Micro-environment and Brain Development Laboratory, Istituto Italiano di Tecnologia, Genova, Italy

[5]Università degli Studi di Genova, Genova, Italy

[6]Dulbecco Telethon Institute, Italy

[7]ITAV-CNRS USR 3505, Toulouse 31106, France

[8]These authors contributed equally

[9]Lead Contact

SUMMARY

Studies in cultured neurons have established that axon specification instructs neuronal polarization and is necessary for dendrite development. However, dendrite formation *in vivo* occurs when axon formation is prevented. The mechanisms promoting dendrite development remain elusive. We find that apical dendrite development is directed by a localized cyclic guanosine monophosphate (cGMP)-synthesizing complex. We show that the scaffolding protein Scribble associates with cGMP-synthesizing enzymes soluble-guanylate-cyclase (sGC) and neuronal nitric oxide synthase (nNOS). The Scribble scaffold is preferentially localized to and mediates cGMP increase in

*Correspondence: maya.shelly@stonybrook.edu.

AUTHOR CONTRIBUTIONS

M.S. conceived the idea for this project and supervised the study. S.P. supervised the FRET experiments. J.S., S.-I.L., A.G., S.P., and M.S. designed the experiments and interpreted the data. J.S., S.-I.L., A.G., and S.P. performed the experiments and analyzed the data. A.W.C. and L.C. assisted with *in utero* gene delivery experiments. T.K. assisted in tissue culture and immunostaining experiments. S.R. assisted with data analysis. G.W. and T.B.H. generated the conditional Scribble mouse line. J.S., S.-I.L., A.G., and M.S. wrote the manuscript with inputs from all the other authors.

DECLARATION OF INTERESTS

The authors declare no competing interests.

SUPPLEMENTAL INFORMATION

Supplemental Information can be found online at https://doi.org/10.1016/j.celrep.2020.03.083.

dendrites. These events are regulated by kinesin KifC2. Knockdown of Scribble, sGC-b1, or KifC2 or disrupting their associations prevents cGMP increase in dendrites and causes severe defects in apical dendrite development. Local cGMP elevation or sGC expression rescues the effects of Scribble knockdown on dendrite development, indicating that Scribble is an upstream regulator of cGMP. During neuronal polarization, dendrite development is directed by the Scribble scaffold that might link extracellular cues to localized cGMP increase.

In Brief

Szczurkowska et al. show that during neuronal polarization, directed mechanisms determine apical dendrite development in embryonic pyramidal neurons. The scaffolding protein Scribble assembles a localized cGMP-synthesis complex in dendrites. The complex is necessary for apical dendrite development in the embryonic hippocampus.

Graphical Abstract

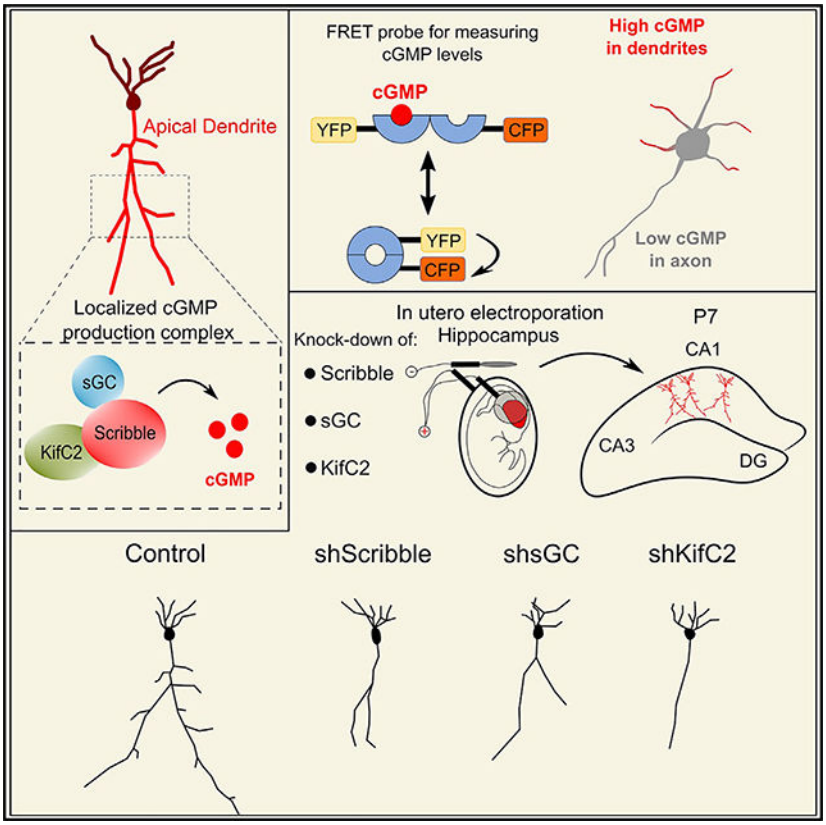

INTRODUCTION

An essential early event in mammalian embryonic brain development is neuronal polarization, in which distinct axonal and dendritic compartments are formed. Axons and dendrites inherently differ in the molecular composition of their cytoplasm, cytoskeleton, and plasma membrane. These differences underlie the unique morphology and function of the axonal and dendritic compartments and are responsible for directed information flow in

the brain. How polarity arises from seemingly equivalent neurites remains an outstanding question.

Specification of the axon has dominated studies on neuron polarization, yielding an understanding of the molecular events underlying axonal identity—specification and growth (Arimura and Kaibuchi, 2007; Barnes et al., 2007; Cheng et al., 2011a, 2011b; Da Silva et al., 2005; de Anda et al., 2005; Dotti and Banker, 1987; Dotti et al., 1988; Inagaki et al., 2001; Jacobson et al., 2006; Jiang et al., 2005; Kishi et al., 2005; Shelly et al., 2007, 2010; Shi et al., 2003; Toriyama et al., 2006; Yoshimura et al., 2005). Much effort has also been directed toward elucidation of the mechanisms that control late events in dendrite morphogenesis—growth, branching, and structural plasticity (Jan and Jan, 2010; Parrish et al., 2007; Tran et al., 2009; Zipursky and Grueber, 2013; Zoghbi, 2003). However, the events in the polarizing neuron that lead to dendrite development are largely unknown.

Preventing axon development in cultured hippocampal neurons produces un-polarized neurons that apparently have no dendrites (Dotti and Banker, 1987; Inagaki et al., 2001; Jacobson et al., 2006; Shelly et al., 2007; Yoshimura et al., 2005), suggesting that in these neurons axon specification precedes and is necessary for dendrite development. The current view for dendrite development in pyramidal progenitors *in vivo* also holds that the axon forms first from one neurite of the multipolar neuron (Namba et al., 2014). The cells then form a leading process and the remaining neurites are removed. Apical dendrite polarity is subsequently established from the leading process of the bipolar neuron. Our findings and other work, however, suggest that *in vivo*, apical dendrite development might be independently directed during or after axon formation by localized intrinsic mechanisms. Although the majority of cortical progenitors develop the axon from the multipolar neuron, in many cells, leading process and polarity establishment preceded trailing process formation (Namba et al., 2014). Moreover, knockdown of determinants for axon formation did not interfere with leading process or apical dendrite development (Barnes et al., 2007; Kishi et al., 2005; Shelly et al., 2007; Yi et al., 2010) suggesting that the apical dendrite can form even in the absence of axon development. Nevertheless, the underlying mechanisms for apical dendrite development have remained elusive.

We have previously shown that axon formation in cultured hippocampal neurons is promoted by elevation of cyclic AMP (cAMP) in a single neurite (Cheng et al., 2011b; Shelly et al., 2007, 2010), followed by a cAMP decrease in the remaining neurites. Together, these events ensure the formation of a single axon. Changes in cAMP were accompanied by opposite changes in cyclic guanosine monophosphate (cGMP), resulting in cGMP increase in the non-axon-forming neurites through an unknown mechanism.

In this study, we found that apical dendrite development is directed by a localized cGMP-synthesizing complex. We show that the scaffold protein Scribble (Bilder and Perrimon, 2000; Moreau et al., 2010; Richier et al., 2010) recruited the cGMP-synthesizing enzymes soluble-guanylate-cyclase (sGC) and neuronal nitric oxide synthase (nNOS). The associations within the complex were necessary for the generation of distinctly higher cGMP levels in dendrites. Furthermore, the complex was necessary for CA1 apical dendrite development. Together with our unpublished observations (unpublished data), we

demonstrate that the Scribble scaffold mediates signals of extracellular cues to localized cGMP increase to promote apical dendrite development during neuronal polarization.

RESULTS

A cGMP Production Scaffold Associates with and Is Necessary for Apical Dendrite Development

The localized production of cGMP might result from the assembly of sGC and nNOS on a common scaffold within neurites and drives their development into dendrites. Our analysis of localized mRNA profiles in the synaptic neuropil of the CA1 region of the hippocampus (from Cajigas et al., 2012), showed a prominent dendritic localization of the nNOS adaptor protein NOS1AP (C-terminal PDZ ligand of nNOS, CAPON) (Carrel et al., 2009; Jaffrey et al.,1998, 2002) that mediates the association of Scribble with nNOS. We analyzed the expression of several known neuronal polarization proteins together with cGMP production enzymes in the stratum oriens (SO) versus stratum radiatum (SR) of rat CA1 at embryonic day 20 (E20). Scribble, nNOS, and sGC-β1 were enriched in the SR, where the apical dendrites of CA1 pyramidal neurons are located (Figure 1A). In contrast, axon determinants (pGSK-3β, pTau, and LKB1) showed enrichment in the SO. We predicted that Scribble serves as a scaffold for assembling a sGC-nNOS complex for cGMP production in dendrites. We determined whether sGC associates with Scribble in the embryonic brain. Co-immunoprecipitation (coIP) from E18 rat brain lysates showed that Scribble associated with the sGC-β1 subunit, the predominant form in the brain (Figure 1B, left), and with nNOS (Figure 1B, right). Immunohistochemical analyses in CA1 pyramidal neurons at post-natal day 7 (P7) showed that both Scribble and sGC-β1 associated with apical dendrites (Figures 1C, arrows, and 1D). These findings showed that Scribble and sGC form a complex and that their expression is associated with apical dendrites in developing pyramidal neurons.

We examined the effect of deleting Scribble on apical dendrite development in CA1 pyramidal neurons in Scribble-$^{Flox/Flox}$ mice (Hartleben et al., 2012) mediated by Emx1^{Cre} recombination (Gorski et al., 2002) to delete Scribble in pyramidal progenitors in the forebrain. Loss of Scribble from Emx1$^{Cre/+}$;Scribble$^{fl/fl}$ hippocampus was confirmed by immunoblotting (Figure 1E). CA1 pyramidal neural progenitors were labeled with dTomato by *in utero* electroporation at E15.5 in wild-type (WT), heterozygous, or homozygous littermates (Figure 1F). At P7, neurons from homozygotes had significant reduction in apical dendrite length and branching compared to WT littermates, whereas heterozygotes had an intermediate phenotype (Figures 1F and 1G). These findings with Scribble deletion demonstrated that the Scribble scaffold is necessary for apical dendrite development in the embryonic CA1.

We also examined dendrite formation in cultures of hippocampal neurons from WT, heterozygous, or homozygous littermates for Scribble deletion (Figures 1I–1L; 5 DIV). Homozygous deletion resulted in a significant reduction in dendrite number per cell compared to WT, whereas heterozygous deletion had an intermediate effect (Figure 1J). Scribble deletion caused an increase in the cell population with only 0–2 dendrites and a decrease in cells with more than 3 dendrites (Figure 1K). Scribble deletion also reduced individual dendrite length (Figure 1L) while slightly increasing axon formation and length

(Figures 1J and 1L). These findings showed that Scribble is necessary for dendrite formation in cultured neurons.

Scribble Association Is Necessary for sGC Dendritic Localization and cGMP Increase

We mapped the sGC-β1 binding site in Scribble by using Scribble mutants with specific domains deleted (Figure 2A) following co-expression of FLAG-sGC-β1 and hemagglutinin (HA)-Scribble mutants in HEK293 cells. Scribble contains N-terminal leucine-rich repeats (LRRs) and four PDZ domains separated by an unassigned intermediate region (IMR) (Figure 2A). We found that the Scribble-sGC-β1 association was mediated mainly by the IMR domain of Scribble because isolated IMR (IMR) interacted with sGC-β1 (Figure 2B), whereas internal deletion of IMR (DIMR) led to a significant reduction in sGC-β1 association (Figure 2C). To determine whether IMR was the critical interface between Scribble and sGC-β1, we expressed increasing amounts of the IMR domain and examined its effect on full-length Scribble and sGC-β1 association (Figure 2D). Expressing IMR in a dose-dependent manner led to decreased recovery of the sGC-β1-Scribble complex (Figure 2D). Together, these findings showed that sGC associated with Scribble and that the Scribble IMR domain mediated their interaction. In our subsequent experiments, we used overexpression of the IMR domain to competitively disrupt the association of endogenous Scribble and sGC-β1.

We asked whether the association of sGC with Scribble is necessary for the regulation of cGMP in developing neurons. We designed a measurement for baseline cGMP in cultured hippocampal neuronsby by using a cGMP FRET sensor, cGi-500 (Russwurm et al., 2007) (Figures S2A and S2B, open circles). The FRET signal from cGi-500 decreases as cGMP levels increase (Figure S2A). To test whether our FRET measurement reliably reflects changes in cGMP, we measured changes in somatic cGMP upon up- or downregulation of sGC. To overexpress sGC we reconstructed sGC by co-transfecting sGC-α1 and -β1 subunits. To knock down sGC-β1, we used ShsGC#3 (Figure 5C). Reflecting the cGMP decrease upon sGC-β1 knockdown, normalized FRET signals (YFP-FRET/YFP total) for sGC-β1-shRNA cells were scattered above those for control (Figures 2F and S2B, blue symbols), whereas there was a decrease in somatic FRET for α1- and β1-sGC co-transfected cells (Figure 2G), indicating that cGMP increased compared to the control. Overexpression of nNOS also elevated cGMP (Figure 2G). These findings demonstrated that our FRET assay accurately reflects cGMP changes upon genetic manipulations of the cGMP enzymes sGC and nNOS.

To test the role of the Scribble-complex in cGMP regulation, we determined the effects of shRNA-mediated Scribble knockdown on cGMP levels in cultured hippocampal neurons transfected with cGi-500 (ShScrib#4; Figures 5A and 5B, arrowhead). To further test whether the sGC association mediated the Scribble effect, we overexpressed IMR (Figure 2D) to disrupt the endogenous Scribble-sGC interaction and quantified effects on cGMP levels. Normalized FRET for ShScrib#4-expressing cells (Figure 2E) were scattered above those for control-short hairpin RNA (shRNA) (Figure S2B, black symbols), similar to sGC-β1-shRNA, indicating somatic cGMP decrease upon Scribble knockdown. The difference in FRET showed that ~80% of Scribble-shRNA- or IMR-transfected neurons (Figure 2F)

exhibited somatic FRET increase compared to control mean, reflecting a cGMP decrease. These findings showed that Scribble assembles a complex for cGMP increase by sGC association.

We next examined whether the association of Scribble with sGC was necessary for generating higher cGMP levels in dendrites. First, we measured normalized FRET signals in each dendrite and the axon of each control neuron (Figures 2H–2J) at 3–4 days *in vitro* (DIV) when neuronal polarization is complete. Quantification of the difference between normalized FRET of each dendrite in each cell to the axon in the same cell revealed three distinct neuronal groups (Figures 2I and 2J): (A) when most or all dendrites had higher cGMP than the axon, (B) when the axon had higher cGMP than most of the dendrites, and (C) when there was no bias in cGMP distribution between the axon and dendrites (Figure 2I). The largest percentage of control neurons had higher cGMP in dendrites (A) than the axon. Neurons with higher cGMP in the axon (B) or those exhibiting no preferential cGMP distribution (C) occurred significantly less (Figure 2J). Furthermore, upon Scribble knockdown (Figures 2H–2J), we found a decrease in the percentage of cells with higher cGMP in dendrites (A) and an increase in cells with the opposite tendency (B) or no preferential cGMP distribution (C) (Figure 2J). These findings showed that Scribble is necessary for increased cGMP generation in dendrites.

To determine whether the Scribble complex is present preferentially in dendrites, we quantified Scribble and sGC localization in axons versus dendrites in cultured hippocampal neurons immunostained for Scribble, sGC-β1, or nNOS, together with neuronal (Tuj-1), dendritic (MAP2), or axonal (smi-312) markers. At 5 DIV, when neuronal polarization is complete and dendrites have formed, we found significantly higher levels of normalized Scribble, sGC-β1, and nNOS immunofluorescence in dendrites (with high MAP2; Figures S3A–S3C) than in axons (with high smi-312). We also examined Scribble and sGC-β1 localization at 2 DIV, when approximately 50%–70% of cells have formed an axon, whereas remaining cells have not yet polarized (Figure S3D). We found that higher levels of normalized Scribble and sGC-β1 were present in the non-axonal neurites (high MAP2) than in nascent axons (high smi-312) in newly polarized neurons (Figure S3E). However, Scribble and sGC-β1 were equally distributed among all neurites in neurons prior to axon polarization (Figures S3D, bottom panel, and S3F). Immunoblotting of 2 DIV or 5 DIV cultured neuronal lysates showed that Scribble had higher expression at 2 DIV than at 5 DIV (Figure S3G), suggesting that during neuronal polarization *in vitro*, Scribble plays an important role in initial dendrite development. These findings showed that Scribble and sGC are localized to dendrites in mature neurons and that this preferential localization occurs at a time when dendrites are formed.

Finally, we examined whether Scribble regulates the polarized presence of cGMP in dendrites by regulating the dendritic localization of sGC. Knocking down Scribble or disrupting its association with sGC by overexpressing IMR prevented the dendritic enrichment of sGC and nNOS (Figures S3H–S3J), consistent with the prevention of increased cGMP in dendrites upon Scribble knockdown (Figures 2H–2J). Thus, the association with Scribble was necessary for the dendritic localization of sGC and, subsequently, for the preferred cGMP generation in dendrites.

Scribble-sGC Association Is Necessary for Apical Dendrite Development

If localized cGMP signaling is necessary for dendrite development and if localized cGMP synthesis requires Scribble-sGC association, Scribble knockdown or disruption of the Scribble-sGC complex should impair dendrite development. We examined whether the requirement for Scribble in apical dendrite development in the embryonic hippocampus (Figures 1F–1H) is mediated by sGC association and its downstream actions. We downregulated Scribble or sGC-β1 and interfered with the Scribble-sGC association by overexpressing IMR in rat CA1 pyramidal neurons by *in utero* electroporation at E17.5 (Figure 3A; dTom fluorescence-based reconstructions). These manipulations significantly reduced apical dendrite length and branching with abnormally simpler and shorter dendrites compared to control neurons (Figure 3A). Quantification of total apical dendrite length in Scribble- or sGC-β1-shRNA or IMR-transfected neurons showed a reduction in apical dendrite growth (Figures 3C, 3E, and 3G). Scribble knockdown also reduced the length of the primary branch of the apical dendrite (excluding secondary, tertiary, and further braches) (Figure 3L). Quantification of total apical dendrite branch points showed a reduction compared to control (Figures 3D, 3F, and 3H).

The defects in apical dendrite development upon Scribble knockdown were fully rescued by co-expressing WT human Scribble (resistant to rat shRNAs; Figures 3B, 3I, and 3J). Furthermore, we tested whether Scribble knockdown defects were rescued by human Scribble-ΔIMR, predicting that ΔIMR should not rescue these defects. Co-expression of ΔIMR with ShScrib#4 (in effect knockin of ΔIMR) resulted in a complex phenotype with a severely shortened primary branch of the apical dendrite that, however, exhibited abnormally excessive lateral branching (Figure 3K, arrow). Although the primary branch of the apical dendrite was shorter with ΔIMR than with Scribble knockdown (Figure 3L), quantification of total apical dendrite length and branching appeared as in control neurons because of its excessive lateral branching (Figures 3I and 3J). These findings underscored the critical role of the IMR domain in apical dendrite development by mediating the Scribble-sGC association. The aberrant branching upon ΔIMR knockin might result from dissociation of the Scribble-sGC complex and its subsequent disassociation from Semaphorin3A-signaling (unpublished data). These findings demonstrated that the Scribble cGMP-production complex is a critical regulator of apical dendrite development in the embryonic CA1.

Scribble knockdown effects were specific to apical dendrites, whereas basal dendrite growth and branching was not reduced (Figure 4). Knockdown of sGC-β1 or disruption of the Scribble-sGC association by expressing IMR also did not reduce basal dendrite length (Figures 4A and 4B) or branching (Figures 4A and 4C). These findings were consistent with the preferred association of Scribble and sGC-b1 with apical dendrites (Figures 1A, 1C, and 1D). Furthermore, we found that Scribble knockdown not only resulted in specific defects in apical dendrites (Figure 3) but also promoted basal dendrite development (Figure 4). Re-expression of Scribble following its knockdown fully rescued apical dendrite defects (Figures 3B, 3I, 3J, and 3L) and increased basal dendrite development (Figure 4). It is possible that following Scribble knockdown, cGMP-production enzymes no longer localize preferentially to the apical dendrite and are instead evenly re-distributed among apical and

basal dendrites. Overexpression of Scribble might result in a similar uniform distribution of cGMP. Both of these manipulations might promote basal dendrite development.

We also examined whether Scribble regulates dendrite formation by sGC association in cultured hippocampal neurons. At 5 DIV, knockdown of Scribble (ShScrib#4; Figures 5D–5F) or sGC-β1 (ShsGC#1; Figures 5D, 5H, and 5I) resulted in a significant reduction in dendrite number per cell, whereas after transfection with ShScrib#1 or ShsGC#2, shRNAs with moderate efficacy (Figures 5A–5C) produced a moderate reduction (Figures 5D–5F and 5H–5I). IMR expression also resulted in a significant reduction in dendrite number (Figures 5K–5M). Furthermore, Scribble or sGC-β1 knockdown or IMR overexpression reduced individual dendrite length (Figures 5G, 5J, and 5N) but slightly increased axon formation and length (Figures 5D, 5E, 5G, 5H, 5J, 5L, and 5N). These findings suggest that the promotion of dendrite formation by Scribble is mediated by sGC association and activity. The reduction in dendrite number without affecting neuron polarization or axon formation is consistent with a specific role of the Scribble complex in dendrite development.

The Scribble Scaffold Is an Upstream Regulator of cGMP Activity

To determine if the critical role of Scribble in dendrite development is attributed to cGMP, we attempted to rescue Scribble knockdown defects by elevating cGMP activity. First, we tested whether local presentation of a cGMP analog can rescue the effects of Scribble knockdown or IMR expression on dendrite formation in cultured neurons. Neurons transfected with ShScrib#4 or IMR were plated on stripes of a membranepermeable analog of cGMP (F-cGMP) or control BSA. Dendrite formation was quantified at 5 DIV in polarized neurons with their soma located on the stripe boundary according to their initiation “on” or “off” stripe regions (Figures 6A–6D). There was a significant reduction in dendrite number in neurons transfected with ShScrib#4 or IMR plated onto control BSA stripes (Figures 6A–6D). In contrast, in neurons expressing ShScrib#4 or IMR and plated on F-cGMP stripes, we found an increase in dendrite number per cell (Figure 6B) and in the percentage of cells with more than 3 dendrites (Figure 6D). Importantly, an increase in dendrite number occurred significantly more on the F-cGMP stripe (side of soma in direct contact with F-cGMP; Figure 6C), which shows that localized cGMP increase rescued dendrite formation after Scribble knockdown or disruption of sGC association (IMR).

We also examined if increased cGMP production by sGC overexpression rescued dendrite development defects following Scribble knockdown *in vivo*. Reconstructed sGC (by co-expressing sGC-α1 and -β1) rescued apical dendrite development defects upon Scribble knockdown (Figures 6E–6G), with increased total length (Figure 6F) and branching (Figure 6G). Re-expression of sGC (sGC-α1 and -β1) following Scribble knockdown also promoted basal dendrite development (Figure 4). This possibly resulted from mis-localization of the overexpressed sGC to and cGMP elevation in basal dendrites, promoting their development.

Our rescue experiments supported the idea that the critical role of Scribble in dendrite development is to elevate cGMP.

Kinesin KifC2 Interacts with Scribble and Is Necessary for cGMP Regulation and Apical Dendrite Development

How might the cGMP complex localize to dendrites? Our findings showed that the complex is excluded from the nascent axon and is preferentially localized to future dendrites (Figures S3D–S3G). Kinesin-mediated transport might restrict Scribble to the somatodendritic compartment. We determined the expression of several kinesins in E18 rat brain lysates. Among others, Kif17 (Yin et al., 2011) and KifC2 (Hanlon et al., 1997; Saito et al., 1997) that mediate dendritic transport were expressed in the embryonic brain (Figure 7A). coIP showed that Scribble associated with KifC2 in embryonic brain lysates (Figure 7B; Figure S4). We, thus, examined whether the Scribble-KifC2 association was necessary for the dendritic localization of Scribble, for the regulation of cGMP in dendrites, and for dendrite development.

First, we determined whether KifC2 association was necessary for dendritic localization of Scribble. We quantified normalized Scribble signal in the axon versus dendrites in ShKifC2#4-transfected cultured neurons (Figure 7C; Figure S5A). There was a significant decrease in the dendritic localization of Scribble upon KifC2 knockdown (Figures S5B and S5C). Together with the preferential neuritic localization of Scribble and its exclusion from the nascent axon (Figures S3D–S3F), these findings suggest that in cultured hippocampal neurons, KifC2 might regulate Scribble localization in future dendrites following axon formation.

Next, we investigated whether the role of KifC2 in the dendritic localization of Scribble was reflected in increased cGMP in dendrites. We measured relative cGMP between the axon and dendrites in neurons co-transfected with the cGi-500 FRET probe and ShKifC2#4 (Figures 7D–7F). We found a significant decrease in the percentage of cells with higher cGMP in dendrites upon KifC2 knockdown than in the control and an increase in cells with opposite cGMP distribution or no differential cGMP between the axon and dendrites (Figures 7E and 7F). Somatic cGMP also decreased upon KifC2 knockdown (Figure S6). These findings demonstrated that KifC2 has a critical role in the localization and function of the Scribble-cGMP complex in dendrites.

Next, we determined whether the effects of KifC2 on the dendritic localization and function of Scribble are required for dendrite development. CA1 pyramidal neurons transfected *in utero* with ShKifC2#4 and examined at P7 had a significant reduction in apical dendrite length and branching (Figures 7G–7I). To examine whether the critical role of KifC2 in dendrite development is mediated by Scribble association and cGMP regulation, we determined whether defects in apical dendrite development following KifC2 knockdown are rescued by Scribble expression or by elevation of cGMP production by sGC expression. Co-expression of WT Scribble or sGC (sGC-α1 and -β1) with ShKifC2#4 rescued apical dendrite defects (Figures 7G–7I), with an increase in total length (Figure 7H) and branching (Figure 7I). Importantly, knockdown of Kif17, a kinesin that is expressed in the embryonic brain (Figure 7A) and that also mediates dendritic transport (Yin et al., 2011), had no effect on apical dendrite development (data not shown), which demonstrates the specificity of our findings with KifC2.

KifC2 downregulation in cultured neurons resulted in significant reduction in dendrite number compared to the control (Figures 7J–7L). KifC2 knockdown also reduced individual dendrite length (Figure 7M) but increased axon formation and length (Figures 7K and 7M). These findings are consistent with Scribble and sGC manipulations and show that KifC2 is a critical regulator of cGMP and dendrite development, likely mediated by Scribble localization. These findings showed that the KifC2-Scribble association was necessary for the dendritic localization of Scribble, for cGMP generation in dendrites, and for dendrite development.

DISCUSSION

The view that axon specification precedes and instructs neuronal polarization and is necessary for dendrite development is based primarily on findings in cultured neurons. This idea prevailed because in these neurons, when axon development is prevented, the neurons are un-polarized and apparently have no dendrites. This notion is supported by recent findings *in vivo* where the axon is specified first from one neurite of the multipolar neuron in majority of pyramidal progenitors (Namba et al., 2014). However, prevention of axon formation in developing pyramidal neurons *in vivo* does not interfere with the formation of the leading process and the subsequent development of the apical dendrite (Barnes et al., 2007; Kishi et al., 2005; Shelly et al., 2007; Yi et al., 2010). These findings suggest that dendrite development can be independently regulated by localized intrinsic signaling. In this study and our unpublished observations (unpublished data), we demonstrated that a complex assembled on the scaffold protein Scribble binds and links cGMP production enzymes to the extracellular Semaphorin3A (Sema3A) cue at the apical dendrite to promote its development.

A cGMP Scaffold Assembled in Dendrites Is Necessary for Dendrite Development

Our findings showed that Scribble forms a functional complex with sGC and is a critical regulator of dendrite formation through cGMP increase. In the non-polarized neuron *in vitro*, Scribble and sGC were equally expressed among all neurites. Once the nascent axon began to form, Scribble became restricted to the remaining neurites. Importantly, sGC demonstrated a similar tendency, possibly by its association with Scribble. Dendrites had distinctly higher cGMP levels than the axon, and this preferential cGMP distribution was Scribble dependent. Disruption of the complex prevented dendritic localization of sGC, causing a reduction in dendritic cGMP and dendrite number. Moreover, in developing CA1 pyramidal neurons *in vivo*, Scribble and sGC expression were enriched at the apical dendrite.Scribble knockdown or deletion in the embryonic hippocampus resulted in severe defects specifically in apical dendrite development. The knockdown of sGC-β1 or interfering with its association with Scribble by manipulations of the IMR domain mimicked these effects.

In vivo, the complex for cGMP production might assemble at the leading process independently from axon formation to mediate apical dendrite development. Scribble and associated proteins have been shown to be expressed in postsynaptic dendritic spines and in presynaptic terminals (Moreau et al., 2010; Richier et al., 2010; Sun et al., 2009; Wang et al.,

2011). Similarly, sGC and nNOS have both presynaptic and postsynaptic functions (Jaffrey et al., 1998, 2002; Wang et al., 2011). Although our investigations showed preferential dendritic localization and function of the Scribble scaffold, we also detected the complex presence in the axon. It is, therefore, possible that Scribble also has axonal functions during neuronal polarization or in the mature neuron.

Kinesin-Mediated Mechanism for Dendritic Localization of the Scribble Scaffold

It is widely accepted that kinesin-driven transport regulates axon and dendrite polarization, but only a few studies have provided evidence for this idea (Horiguchi et al., 2006; Jacobson et al., 2006; Petersen et al., 2014; Shi et al., 2004). We found that the embryonic brain expressed several kinesins known to be involved in axon- or dendrite-directed trafficking. These included the C-terminal motor KifC2 that is thought to mediate dendritic transport (Hanlon et al., 1997; Saito et al., 1997). The embryonic brain expresses KifC2 as early as E14 (Saito et al., 1997), consistent with our findings, although its expression increases in mature neurons in the early postnatal brain. KifC2 localizes to dendrites of pyramidal neurons but was not found in axons (Saito et al., 1997). We found that the Scribble and KifC2 association was necessary for dendritic localization of Scribble, for increased cGMP in dendrites, and for dendrite formation *in vitro* and *in vivo*, which are findings consistent with those for Scribble and sGC manipulations. Although KifC2 might also have Scribble-independent roles in neuronal development, our findings underscore the importance of the Scribble-KifC2 association in the dendritic localization of the Scribble scaffold and its subsequent role in dendrite development. In support of this notion, we found that overexpression of Scribble or functional sGC rescued the defects in dendrite development upon KifC2 knockdown *in vivo*.

Following axon specification, Scribble and sGC were excluded from the axon and were restricted to the neurites. How might KifC2 mediate neuritic restriction of Scribble scaffold following axon specification? In mature neurons, axon and dendrites exhibit a striking difference in the orientation of their microtubules (MTs): axonal MTs are pointed plus-end-out, whereas dendrites exhibit a mixed polarity (Hirokawa et al., 2010). In the mature neuron, the C-terminal motor KifC2, which travels toward MT minus-ends, should not enter the axon and should restrict the somatodendritic localization of Scribble. This simple scenario, however, cannot apply to the polarizing neuron. Before polarization and right after axon specification, MTs in all neurites, including the nascent axon, display identical polarity with their plus-ends pointing out (Jacobson et al., 2006). Nevertheless, axonal and dendritic MTs at this stage have unique properties, enabling select kinesin trafficking to or exclusion from the nascent axon. Kif5C (Arimura et al., 2009; Jacobson et al., 2006; Nakata and Hirokawa, 2003), Kif3A (Shi et al., 2004), and GAKIN/Kif13B (Horiguchi et al., 2006), might selectively traffic to the nascent axon, whereas Kif1A showed equal distribution in all neurites. It is unclear what MT quality enables this distinction prior to MT polarity establishment. The presence of distinct axonal or dendritic MT-associated proteins (MAPs), MT dynamics (Hirokawa et al., 2010), the interplay between kinesin and dynein motors in binding cargo (Franker et al., 2016), or post-translational modifications of tubulin might regulate selective kinesin transport. Similar recognition of unique MT properties might make the nascent axon not permissive to KifC2, restricting it and the associated Scribble scaffold

to the neurites. The subsequent neuritic increase in cGMP might promote their dendrite development.

Scribble Might Link Extracellular Cues to cGMP in Apical Dendrite Development

Our study demonstrates that dendrite development results from a localized cGMP production complex. The reduction in dendrite number without preventing neuron polarization or axon development following knockdown of the Scribble-cGMP complex *in vitro* is consistent with its specific role in dendrite development. The exclusion of the Scribble-cGMP scaffold from the nascent axon will ensure the polarized production of cGMP in the neurites, suppressing their axon fate and promoting dendrite development. Scribble knockdown or manipulation of its association with sGC might result in the selective disassembly of the cGMP complex in dendrites and subsequent defects in dendrite development. In support of this idea, we found that local cGMP elevation or increased sGC activity rescued the dendrite defects induced by Scribble knockdown. These findings demonstrate that Scribble regulates dendrite formation locally in the neurites upstream of cGMP activity.

Prevention of axon formation *in vivo* does not interfere with bipolar polarity establishment, leading process formation, or apical dendrite development (Barnes et al., 2007; Kishi et al., 2005; Shelly et al., 2007; Yi et al., 2010). In the developing brain, spatially organized extrinsic cues may mediate leading process polarization and apical dendrite development by acting on localized intrinsic signaling. Nevertheless, deletion of many extracellular cues and their receptors did not identify a particular factor that might mediate axon and dendrite polarization *in vivo* (Behar et al., 1996; Crowley et al., 1994; Da Silva et al., 2005; Jones et al., 1994; Klein et al., 1993; Polleux et al., 1998; Smeyne et al., 1994; Sosa et al., 2006; Yoshimura et al., 2005). Our unpublished observations (unpublished data) show that the Scribble complex also associated with the Sema3A co-receptor PlexinA3. We found that this interaction was necessary for Sema3A-mediated cGMP increase and apical dendrite development. By associating with intracellular cGMP-production machinery on one hand and with Sema3A-signaling complex on the other, Scribble might mediate extracellular cues for local rise in cGMP levels to promote apical dendrite development.

STAR★METHODS

LEAD CONTACT AND MATERIALS AVAILABILITY

Further information and requests for resources and reagents should be directed to and will be fulfilled by the Lead Contact, Maya Shelly (maya.shelly@stonybrook.edu). This study did not generate new unique reagents.

EXPERIMENTAL MODEL AND SUBJECT DETAILS

Rats and mice were used according to protocols approved by the Institutional Animal Care and Use Committees at Stony Brook University. Timed pregnant Sprague Dawley rats were delivered from Charles River. $Emx1^{Cre/+}$;$Scribble^{fl/fl}$ mouse line were generated by crossing the $Emx1^{cre}$ mouse line (Jackson laboratory) and the $Scribble^{Flox/Flox}$ mouse line (Hartleben et al., 2012) (kindly provided by Dr. Tobias B. Huber, University Medical Center Freiburg,

Germany). Control and experimental pups at P7 (males and females) were obtained from the same litter.

METHOD DETAILS

Plasmid constructs and shRNAs—To suppress endogenous rat Scribble, we generated three shRNA sequences, ShScrib#1, ShScrib#2, and ShScrib#3. The target sequences were selected using a web-based program, siRNA at Whitehead. Overhang sequences and linker sequences were added to clone the sequences into the PRNT U6.1 vector (Genescript). The sequences of oligomers are the following:

ShScrib#1; 5′-GATCCCAGAGATCTTGAAGTGCTTCTTTTGATATCCGAAGAAGCACTTCAAGATCTCTTTTTTTCCAAA-3′;

ShScrib#2; 5′-GATCCCAGGGAGAGATTTAAGCAGGTTTTGATATCCGAACCTGCTTAAATCTCTCCCTTTTTTTCCAAA-3′;

ShScrib#3; 5′-GATCCCGCCCTGTAGTCAAACTTCTTTTTGATATCCGAAAGAAGTTTGACTACAGGGCTTTTTTTCCAAA-3′.

Importantly, for the FRET experiments, these shRNA sequences were cloned into PRNT U6.1 expression vector that also drives expression of dTom, otherwise, the vector expressed EGFP. We generated three shRNA sequences for rat KifC2, as follows:

ShKifC2#1; 5′-GATCCCGAAGTCTACTCAGCTCTTCTTTTGATATCCGAAGAAGAGCTGAGTAGACTTCTTTTTTCCAAA-3′;

ShKifC2#2; 5′-GATCCCGCAAGAGCTGACTTGTTACTGTTTGATATCCGACAGTAACAAGTCAGCTCTTGTTTTTTCCAAA-3′;

ShKifC2#3; 5′-GATCCCGTGTCAGTACTGAGAGAAGAATTGATATCCGTTCTTCTCTCAGTACTGACACTTTTTTTCCAAA-3′.

The shRNAs targeting rat sGC-β1 subunit (ShsGC#1 and ShsGC#2) were previously described (Shelly et al., 2010).

To generate the pCAGJC-HA-rat Scribble, Scribble-cDNA corresponding to rat Scribble (GenBank: NP_001178808) was synthesized from total RNA of P1 rat brain by RT-PCR, and cloned into pCAGJC vector. To generate the pCAGJC-HA-hScribble, the cDNA of human Scribble was PCR-amplified from pLNCX-hScribble (a kind gift from Dr. Senthil Muthuswamy, Cold Spring Harbor Laboratory, NY) and cloned into the pCAGJC-HA vector. WT Scribble contains 16 N-terminal leucine-rich repeats (LRRs), followed by four PDZ domains, and separated by an unassigned Intermediate Region (IMR). Scribble mutant forms were generated using PCR procedures, and included those in which the LRR (ΔLRR), LRR and IMR (PDZ/C), or all three domains LRR, IMR and PDZ were deleted (C-term);

variants expressing the isolated LRR (LRR), IMR (IMR), and PDZ domains (PDZs); and mutants in which IMR (ΔIMR), PDZ domains (ΔPDZs), or C-terminal region (ΔC-term), were internally deleted.

To generate the pCAGJC-FLAG-nNOS, the cDNA for rat nNOS was PCR-amplified from pcDNA3.1 nNOS-GFP (a kind gift from Dr. Bonnie Firestein, Rutgers, the State University of New Jersey, Piscataway, NJ). To generate the pCAGJC-FLAG-rat sGC-β1, the cDNA of rat sGC-β1 (GenBank: NM_012769) was PCR-amplified and cloned into pCAGJC-FLAG vector. The cGMP FRET Probe cGi-500 was a kind gift from Dr. Doris Koesling (Ruhr-University Bochum, Germany) and described previously (Russwurm et al., 2007). The pCAGJC and pCAGJC-dTomato were described previously (Shelly et al., 2007). To generate the pCAGJC-HA or pCAGJC-FLAG, we used the nucleotide sequence coding HA tag (YPYDCPDYA) or Flag tag (DYKDDDDK), and cloned into pCAGJC. Rat KifC2 sequence (GenBank: AJ250329.1) was fused to EGFP and cloned into pCAGJC vector.

Primary hippocampal culture and transfection—Cultures of dissociated hippocampal neurons were prepared from either rat or mouse embryos as described previously (Dotti and Banker, 1987; Dotti et al., 1988). Neurons were plated onto a glass coverslip coated with poly-L-lysine (PLL), and cultured for 2 to 5 days. Amaxa nucleofection system (Lonza AG) was used to deliver exogenous genes or shRNAs into primary neurons.

Micro-fabrication and substrate patterning—A silicon wafer was used to generate a template for the poly(dimethylsiloxane) (PDMS) mold and substrates were patterned in parallel stripes of 50 μm width separated by 50 μm gaps. PDMS mold was reversibly sealed on poly-L-lysine-coated glass coverslip, and microchannels formed between the PDMS mold and coverslip were used for microfluidic patterning of membrane permeable F-cGMP analog (Shelly et al., 2017). Fluorescently conjugated BSA served control. Solutions were present in the microchannels for few hours and allowed to dry. The stripe-coated coverslips were washed extensively before plating of dissociated neurons. Dendrite initiation “on” or “off” the stripe was defined for cells with their soma located on the stripe boundary, and quantified by using the preference index (PI = [(% on stripe) - (% off stripe)] / 100%).

Transfection, immunoblotting and immunoprecipitation—HEK293 cells were transfected with plasmid DNA using calcium-phosphate method. 1 to 2 days after transfection, the cells were lysed, and lysates were subjected to immunoprecipitation and immunoblotting.

For detection of endogenous proteins from the embryonic brain, embryonic rat or mice brains were lysed and soluble fractions were subjected to immunoprecipitation and immunoblotting. For preparation of lysates from the stratum oriens (SO) versus stratum radiatum (SR) of rat CA1 region of the hippocampus, these brain regions were dissected at E20.

Immunohistochemistry—Cultured cells were fixed in 4% paraformaldehyde. Following fixation, cells were washed with PBS, permeabilized with 0.05% Triton x-100, and blocked

with PBS containing 10% normal goat serum. Primary antibodies were incubated overnight at 4°C. The cultures were washed and incubated with secondary antibodies for 2 hours.

Brains were fixed in 4% paraformaldehyde and stored in 30% sucrose. Brains were coronally sectioned at 30–60 μm thickness, and mounted onto glass slides. Brain slices were permeabilized for 30 minutes in PBS with 0.3% Triton x-100, and blocked in PBS with 5% normal goat serum and 0.6% Triton x-100. Primary antibodies were incubated for 24 to 48 hours at 4°C. The sections were then washed with PBS with 0.1% Triton x-100 and incubated with secondary antibodies. Slices were also subjected to antigen-retrieval procedure prior to immunostaining.

FRET imaging and analysis—We designed a unique measurement for determining changes in the baseline level of cGMP in cultured hippocampal neurons, resulting from genetic manipulations of Scribble, sGC, or KifC2, using a fluorescence resonance energy transfer (FRET) sensor (Russwurm et al., 2007) for cGMP, cGi-500. The neurons, plated on glass-bottom dishes for live imaging (MatTek Corporation), were co-transfected prior to cell plating by electroporation with a construct encoding the FRET cGMP reporter cGi-500, together with shRNAs or DNA constructs. The FRET measurements were performed at 36 to 48 hr after cell plating, to allow sufficient time for probe and shRNA expressions.

Neurons were imaged with EMCCD camera (Andor Technology PLC, UK), and epifluorescence microscope (Olympus, Center Valley, PA), equipped with a 75-W Xenon lamp and a 60x NA 1.42 objective (Olympus). FRET measurements were performed by CFP excitation with a band pass (440/20 nm) excitation filter, and simultaneous measurement of the fluorescence emission of CFP and YFP, using a dual view beam splitter equipped with a band pass (480/40 nm) emission filter for CFP and a band pass (530/40 nm) emission filter for YFP. The intensity of the light source and the exposure times, were kept constant for all measurements for somatic FRET, or FRET measurement in the axons and dendrites, respectively. FRET signal was determined by YFP fluorescence measured upon CFP excitation (YFP-FRET). Because the FRET signal (YFP-FRET) in each cell would depend on the level of probe expression in that cell, FRET values were normalized to total YFP levels, determined upon YFP excitation (YFP-total), with the assumption that total YFP levels (YFP-total) reflect the level of probe expression in each cell. To measure YFP-total, YFP was excited using a band pass (515/20 nm) excitation filter.

For somatic FRET measurements, for each cell, we measured the mean fluorescence intensity over the cell area, for each channel: YFP-total obtained upon YFP excitation and measurement of YFP emission, CFP donor obtained upon CFP excitation and measurement of CFP emission, and YFP acceptor obtained upon CFP excitation and measurement of YFP emission. All fluorescence intensities measured were background-subtracted (with background intensity taken from a cell-free region), and were corrected for bleed-through. Baseline somatic cGMP was determined by FRET signals in each control-shRNA or respective control-vector transfected cell, normalized to cGi-500 probe expression level in that cell (YFP-FRET / YFP-total), and presented for all cells with varying probe concentration (YFP-total). This analysis in control-transfected cells enabled to determine a range in which the FRET signals (YFP-FRET) demonstrated a linear correlation with the

levels of probe expression. This linear range of FRET response represents the baseline levels of cGMP in control-transfected cells. To determine the change in cGMP levels following different genetic manipulations, we examined the difference in FRET signals (ΔYFP-FRET/YFP-total) for experimentaltransfected cells compared to respective control-transfected cells, at corresponding levels of probe expression (YFP-total). Importantly, the cGi-500 sensor relaxes its conformation upon cGMP binding, resulting in FRET reduction, whereas reduction in cGMP is reflected in FRET increase (Russwurm et al., 2007).

For FRET measurements in axons and dendrites of individual neurons, normalized FRET signals (YFP-FRET / YFP-total) were determined for all dendrites in each cell (measurements averaged over the entire dendritic length) and the axon (measurement averaged over ~50μm axonal segment, at least 30mm away from the soma), in individual neurons, at 3 to 4DIV, a time when axon specification and formation is complete. Data was presented for each cell, as the difference in normalized FRET signals (ΔYFP-FRET / YFP-total) between dendrites of an individual neuron relative to the axon of that neuron. Following quantification of the difference between normalized FRET signals of each dendrite of individual neurons relative to that of the axon of that neuron, neurons were categorized into three groups: group A, most or all dendrites had lower normalized FRET (higher cGMP) than the axon; group B, most or all dendrites had higher normalized FRET (lower cGMP) than the axon; group C, equal number of dendrites had higher or lower normalized FRET than the axon. The average percentage of cells in each group was quantified in control and experimental neurons.

In Utero Electroporation—Timed-pregnant Sprague Dawley rat at E17.5 or timed-pregnant mouse at E15.5, was anesthetized with isoflurane and its uterine horns were exposed by laparotomy. DNA solution (0.5~1.5 mg/ml) with the dye Fast Green (0.3mg/ml) was injected through the uterine wall into the lateral ventricles of each embryo. We used the triple-electrode probe configuration to target the hippocampus, labeling CA1 pyramidal neural progenitors, as previously described (dal Maschio et al., 2012; Szczurkowska et al., 2016). In brief, a tweezer-type circular electrode was allowed to hold both temporal sides of the embryo head, while a third electrode was placed on top of lateral ventricles at 0° angle with respect to the horizontal plane. The forceps-type electrodes were connected to the positive poles and the third electrode to the negative pole. Five electrical pulses (50 V, 50ms duration at 100ms intervals for rats; 30V, 50ms duration at 1 s intervals for mice) were delivered with a square-wave electroporation generator (model ECM 830, BTX, Inc.). The uterine horns were then returned into the abdominal cavity and the embryos allowed to continue their development. Control and experimental embryos/pups were obtained from the same litter. The shRNA or protein expression constructs were co-transfected with a separate vector pCAGJC-dTomato as a marker. All animal protocols were approved by the Institutional Animal Care and Use Committees of Stony Brook University.

Morphometric analysis—In cultured hippocampal neurons, axons and dendrites were determined by immunostaining and morphology. A Smi-312-positive process that was at least twice longer than every other neurite, was defined as the axon. A primary neuritic process directly extending from the soma of polarized neurons was determined to be a

dendrite based on MAP2 labeling. Only processes longer than 5 mm that were initiated within 5 μm from the soma when branching occurred, and that were positive for MAP2, were considered individual dendrites. For quantitative measurements of Scribble, nNOS or sGC-β1 expression in the dendrites versus the axon, immunofluorescence intensity for the respective proteins was measured in each dendrite or the axon (measurement averaged over the entire neuritic length for the axon and dendrite; taken ~30μm away from the soma for the axon), and was normalized to that of Tuj-1 immunofluorescence, following background subtraction. The expression of dendrite and axon markers, MAP2 and Smi-312, respectively, were similarly quantified in the dendrites and axon.

For morphological analysis of CA1 pyramidal neurons, postnatal (P7) brains were dissected and fixed with 4% paraformaldehyde. Brains were sectioned coronally with a vibratome (Leica, VT1000S) at the level of the hippocampus, and the slices (80 mm) were mounted in Fluoromount G (Southern Biotech, Inc.). For morphometric analysis, confocal images of isolated neurons were acquired with a 40x (N.A. 1.43) oil-immersion objective. For analysis of dendrite number and length, 3D images of entire dendritic arbors were reconstructed from the Z series stacks of confocal images using IMRS 7.3.1 software (Bitplane). Total length and complexity of each process were measured and analyzed using the filament measurement in the software. Dendrite morphology was also measured and analyzed using ImageJ software. 30–90 neurons from multiple sections, from 3–5 brains, were analyzed for each condition. DAPI staining was used for layer determination.

QUANTIFICATION AND STATISTICAL ANALYSIS

Quantification of biochemical analyses of protein immunoblotting (IB) or immunoprecipitation (IP) are based on at least three independent experiments. Data was normalized to total levels of the respective proteins or to β-actin, and quantified as fold change relative to the respective control. Quantification of average Scribble or sGC-β1 immunofluorescence in apical dendrite versus soma compartments in CA1 pyramidal neurons was normalized to that of dTom (n = 12–15 cells), presented as fold change relative to normalized apical dendrite signal. Total apical or basal dendrite length or branch points, or the length of the primary process of the apical dendrite, in CA1 pyramidal neurons was quantified at P7 from at least 35 cells. Axon and dendrite number and length in cultured hippocampal neurons was quantified at 5DIV, from at least 50 cells each from 3–5 cultures. Based on dendrite number, we quantified the percentage of cells that developed only 0–2 dendrites or more than 3 dendrites. Changes in somatic cGMP levels were quantified by the difference in somatic FRET signals (ΔYFP-FRET / YFP-total) relative to respective control from at least 30 cells each from at least 3 cultures. To Quantify the difference in normalized FRET signals (ΔYFP-FRET / YFP-total) between dendrites of individual neurons relative to the axon of that same neuron (signals averaged over the entire dendritic length and ~50μm axonal segment), neurons were categorized into three groups: A, most or all dendrites had lower normalized FRET (higher cGMP) than axon; B, most or all dendrites had higher normalized FRET (lower cGMP) than axon; C, equal number of dendrites had higher or lower normalized FRET than axon. Average percentage of cells in each group was quantified in at least ~80 cells from up to 7 cultures. Student’s t test was used to compare between two

different experimental conditions. One Way ANOVA was used to compare between multiple experimental conditions. *$p < 0.05$; **$p \leq 0.01$; ***$p \leq 0.001$. Error bars represent SEM.

DATA AND CODE AVAILABILITY

This study did not generate any code. All acquired data are available upon request to M.S. (maya.shelly@stonybrook.edu)

Supplementary Material

Refer to Web version on PubMed Central for supplementary material.

ACKNOWLEDGMENTS

We thank Dr. S. Halegoua, Dr. D. Talmage, and Dr. Craig Evinger for critical comments on the manuscript. This work was supported by a grant from NIH, NS084111 (M.S.). T.B.H. was supported by the DFG, Germany (CRC1192, HU 1016/8-2, HU 1016/11-1, HU 1016/ 12-1). We thank Dr. V. Nikolaev (University Medical Center Hamburg-Eppendorf, UKE) for kindly providing the cGMP-FRET reporter cGi-500.

REFERENCES

Arimura N, and Kaibuchi K (2007). Neuronal polarity: from extracellular signals to intracellular mechanisms. Nat. Rev. Neurosci 8, 194–205. [PubMed: 17311006]

Arimura N, Kimura T, Nakamuta S, Taya S, Funahashi Y, Hattori A, Shimada A, Mé nager C, Kawabata S, Fujii K, et al. (2009). Anterograde transport of TrkB in axons is mediated by direct interaction with Slp1 and Rab27. Dev. Cell 16, 675–686. [PubMed: 19460344]

Barnes AP, Lilley BN, Pan YA, Plummer LJ, Powell AW, Raines AN, Sanes JR, and Polleux F (2007). LKB1 and SAD kinases define a pathway required for the polarization of cortical neurons. Cell 129, 549–563. [PubMed: 17482548]

Behar O, Golden JA, Mashimo H, Schoen FJ, and Fishman MC (1996). Semaphorin III is needed for normal patterning and growth of nerves, bones and heart. Nature 383, 525–528. [PubMed: 8849723]

Bilder D, and Perrimon N (2000). Localization of apical epithelial determinants by the basolateral PDZ protein Scribble. Nature 403, 676–680. [PubMed: 10688207]

Cajigas IJ, Tushev G, Will TJ, tom Dieck S, Fuerst N, and Schuman EM (2012). The local transcriptome in the synaptic neuropil revealed by deep sequencing and high-resolution imaging. Neuron 74, 453–466. [PubMed: 22578497]

Carrel D, Du Y, Komlos D, Hadzimichalis NM, Kwon M, Wang B, Brzustowicz LM, and Firestein BL (2009). NOS1AP regulates dendrite patterning of hippocampal neurons through a carboxypeptidase E-mediated pathway. J. Neurosci 29, 8248–8258. [PubMed: 19553464]

Cheng PL, Lu H, Shelly M, Gao H, and Poo MM (2011a). Phosphorylation of E3 ligase Smurf1 switches its substrate preference in support of axon development. Neuron 69, 231–243. [PubMed: 21262463]

Cheng PL, Song AH, Wong YH, Wang S, Zhang X, and Poo MM (2011b). Self-amplifying autocrine actions of BDNF in axon development. Proc. Natl. Acad. Sci. USA 108, 18430–18435. [PubMed: 22025720]

Crowley C, Spencer SD, Nishimura MC, Chen KS, Pitts-Meek S, Armanini MP, Ling LH, McMahon SB, Shelton DL, Levinson AD, et al. (1994). Mice lacking nerve growth factor display perinatal loss of sensory and sympathetic neurons yet develop basal forebrain cholinergic neurons. Cell 76, 1001–1011. [PubMed: 8137419]

Da Silva JS, Hasegawa T, Miyagi T, Dotti CG, and Abad-Rodriguez J (2005). Asymmetric membrane ganglioside sialidase activity specifies axonal fate. Nat. Neurosci. 8, 606–615. [PubMed: 15834419]

dal Maschio M, Ghezzi D, Bony G, Alabastri A, Deidda G, Brondi M, Sato SS, Zaccaria RP, Di Fabrizio E, Ratto GM, and Cancedda L (2012). High-performance and site-directed in utero electroporation by a triple-electrode probe. Nat. Commun. 3, 960. [PubMed: 22805567]

de Anda FC, Pollarolo G, Da Silva JS, Camoletto PG, Feiguin F, and Dotti CG (2005). Centrosome localization determines neuronal polarity. Nature 436, 704–708. [PubMed: 16079847]

Dotti CG, and Banker GA (1987). Experimentally induced alteration in the polarity of developing neurons. Nature 330, 254–256. [PubMed: 3313064]

Dotti CG, Sullivan CA, and Banker GA (1988). The establishment of polarity by hippocampal neurons in culture. J. Neurosci 8, 1454–1468. [PubMed: 3282038]

Franker MA, Esteves da Silva M, Tas RP, Tortosa E, Cao Y, Frias CP, Janssen AFJ, Wulf PS, Kapitein LC, and Hoogenraad CC (2016). Three-Step Model for Polarized Sorting of KIF17 into Dendrites. Curr. Biol 26, 1705–1712. [PubMed: 27265394]

Gorski JA, Talley T, Qiu M, Puelles L, Rubenstein JL, and Jones KR (2002). Cortical excitatory neurons and glia, but not GABAergic neurons, are produced in the Emx1-expressing lineage. J. Neurosci 22, 6309–6314. [PubMed: 12151506]

Hanlon DW, Yang Z, and Goldstein LS (1997). Characterization of KIFC2, a neuronal kinesin superfamily member in mouse. Neuron 18, 439–451. [PubMed: 9115737]

Hartleben B, Widmeier E, Wanner N, Schmidts M, Kim ST, Schneider L, Mayer B, Kerjaschki D, Miner JH, Walz G, and Huber TB (2012). Role of the polarity protein Scribble for podocyte differentiation and maintenance. PLoS One 7, e36705. [PubMed: 22586490]

Hirokawa N, Niwa S, and Tanaka Y (2010). Molecular motors in neurons: transport mechanisms and roles in brain function, development, and disease. Neuron 68, 610–638. [PubMed: 21092854]

Horiguchi K, Hanada T, Fukui Y, and Chishti AH (2006). Transport of PIP3 by GAKIN, a kinesin-3 family protein, regulates neuronal cell polarity. J. Cell Biol 174, 425–436. [PubMed: 16864656]

Inagaki N, Chihara K, Arimura N, Mé nager C, Kawano Y, Matsuo N, Nishimura T, Amano M, and Kaibuchi K (2001). CRMP-2 induces axons in cultured hippocampal neurons. Nat. Neurosci. 4, 781–782. [PubMed: 11477421]

Jacobson C, Schnapp B, and Banker GA (2006). A change in the selective translocation of the Kinesin-1 motor domain marks the initial specification of the axon. Neuron 49, 797–804. [PubMed: 16543128]

Jaffrey SR, Snowman AM, Eliasson MJ, Cohen NA, and Snyder SH (1998). CAPON: a protein associated with neuronal nitric oxide synthase that regulates its interactions with PSD95. Neuron 20, 115–124. [PubMed: 9459447]

Jaffrey SR, Benfenati F, Snowman AM, Czernik AJ, and Snyder SH (2002). Neuronal nitric-oxide synthase localization mediated by a ternary complex with synapsin and CAPON. Proc. Natl. Acad. Sci. USA 99, 3199–3204. [PubMed: 11867766]

Jan YN, and Jan LY (2010). Branching out: mechanisms of dendritic arborization. Nat. Rev. Neurosci. 11, 316–328. [PubMed: 20404840]

Jiang H, Guo W, Liang X, and Rao Y (2005). Both the establishment and the maintenance of neuronal polarity require active mechanisms: critical roles of GSK-3beta and its upstream regulators. Cell 120, 123–135. [PubMed: 15652487]

Jones KR, Fariñas I, Backus C, and Reichardt LF (1994). Targeted disruption of the BDNF gene perturbs brain and sensory neuron development but not motor neuron development. Cell 76, 989–999. [PubMed: 8137432]

Kishi M, Pan YA, Crump JG, and Sanes JR (2005). Mammalian SAD kinases are required for neuronal polarization. Science 307, 929–932. [PubMed: 15705853]

Klein R, Smeyne RJ, Wurst W, Long LK, Auerbach BA, Joyner AL, and Barbacid M (1993). Targeted disruption of the trkB neurotrophin receptor gene results in nervous system lesions and neonatal death. Cell 75, 113–122. [PubMed: 8402890]

Moreau MM, Piguel N, Papouin T, Koehl M, Durand CM, Rubio ME, Loll F, Richard EM, Mazzocco C, Racca C, et al. (2010). The planar polarity protein Scribble1 is essential for neuronal plasticity and brain function. J. Neurosci 30, 9738–9752. [PubMed: 20660256]

Nakata T, and Hirokawa N (2003). Microtubules provide directional cues for polarized axonal transport through interaction with kinesin motor head. J. Cell Biol 162, 1045–1055. [PubMed: 12975348]

Namba T, Kibe Y, Funahashi Y, Nakamuta S, Takano T, Ueno T, Shimada A, Kozawa S, Okamoto M, Shimoda Y, et al. (2014). Pioneering axons regulate neuronal polarization in the developing cerebral cortex. Neuron 81, 814–829. [PubMed: 24559674]

Parrish JZ, Emoto K, Jan LY, and Jan YN (2007). Polycomb genes interact with the tumor suppressor genes hippo and warts in the maintenance of Drosophila sensory neuron dendrites. Genes Dev. 21, 956–972. [PubMed: 17437999]

Petersen JD, Kaech S, and Banker G (2014). Selective microtubule-based transport of dendritic membrane proteins arises in concert with axon specification. J. Neurosci 34, 4135–4147. [PubMed: 24647935]

Polleux F, Giger RJ, Ginty DD, Kolodkin AL, and Ghosh A (1998). Patterning of cortical efferent projections by semaphorin-neuropilin interactions. Science 282, 1904–1906. [PubMed: 9836643]

Richier L, Williton K, Clattenburg L, Colwill K, O'Brien M, Tsang C, Kolar A, Zinck N, Metalnikov P, Trimble WS, et al. (2010). NOS1AP associates with Scribble and regulates dendritic spine development. J. Neurosci. 30, 4796–4805. [PubMed: 20357130]

Russwurm M,Mullershausen F,Friebe A,Jäger R,Russwurm C,andKoesling D (2007). Design of fluorescence resonance energy transfer (FRET)-based cGMP indicators: a systematic approach. Biochem. J 407, 69–77. [PubMed: 17516914]

Saito N, Okada Y, Noda Y, Kinoshita Y, Kondo S, and Hirokawa N (1997). KIFC2 is a novel neuron-specific C-terminal type kinesin superfamily motor for dendritic transport of multivesicular body-like organelles. Neuron 18, 425–438. [PubMed: 9115736]

Shelly M, Cancedda L, Heilshorn S, Sumbre G, and Poo MM (2007). LKB1/STRAD promotes axon initiation during neuronal polarization. Cell 129, 565–577. [PubMed: 17482549]

Shelly M, Lim BK, Cancedda L, Heilshorn SC, Gao H, and Poo MM (2010). Local and long-range reciprocal regulation of cAMP and cGMP in axon/dendrite formation. Science 327, 547–552. [PubMed: 20110498]

Shelly M, Lee SI, Suarato G, Meng Y, and Pautot S (2017). Photolithography-Based Substrate Microfabrication for Patterning Semaphorin 3A to Study Neuronal Development. Methods Mol. Biol 1493, 321–343. [PubMed: 27787862]

Shi SH, Jan LY, and Jan YN (2003). Hippocampal neuronal polarity specified by spatially localized mPar3/mPar6 and PI 3-kinase activity. Cell 112, 63–75. [PubMed: 12526794]

Shi SH, Cheng T, Jan LY, and Jan YN (2004). APC and GSK-3beta are involved in mPar3 targeting to the nascent axon and establishment of neuronal polarity. Curr. Biol 14, 2025–2032. [PubMed: 15556865]

Smeyne RJ, Klein R, Schnapp A, Long LK, Bryant S, Lewin A, Lira SA, and Barbacid M (1994). Severe sensory and sympathetic neuropathies in mice carrying a disrupted Trk/NGF receptor gene. Nature 368, 246–249. [PubMed: 8145823]

Sosa L, Dupraz S, Laurino L, Bollati F, Bisbal M, Cáceres A, Pfenninger KH, and Quiroga S (2006). IGF-1 receptor is essential for the establishment of hippocampal neuronal polarity. Nat. Neurosci 9, 993–995. [PubMed: 16845384]

Sun Y, Aiga M, Yoshida E, Humbert PO, and Bamji SX (2009). Scribble interacts with beta-catenin to localize synaptic vesicles to synapses. Mol. Biol. Cell 20, 3390–3400. [PubMed: 19458197]

Szczurkowska J, Cwetsch AW, dal Maschio M, Ghezzi D, Ratto GM, and Cancedda L (2016). Targeted in vivo genetic manipulation of the mouse or rat brain by in utero electroporation with a triple-electrode probe. Nat. Protoc 11, 399–412. [PubMed: 26844428]

Toriyama M, Shimada T, Kim KB, Mitsuba M, Nomura E, Katsuta K, Sakumura Y, Roepstorff P, and Inagaki N (2006). Shootin1: A protein involved in the organization of an asymmetric signal for neuronal polarization. J. Cell Biol 175, 147–157. [PubMed: 17030985]

Tran TS, Rubio ME, Clem RL, Johnson D, Case L, Tessier-Lavigne M, Huganir RL, Ginty DD, and Kolodkin AL (2009). Secreted semaphorins control spine distribution and morphogenesis in the postnatal CNS. Nature 462, 1065–1069. [PubMed: 20010807]

Wang T, Liu Y, Xu XH, Deng CY, Wu KY, Zhu J, Fu XQ, He M, and Luo ZG (2011). Lgl1 activation of rab10 promotes axonal membrane trafficking underlying neuronal polarization. Dev. Cell 21, 431–444. [PubMed: 21856246]

Yi JJ, Barnes AP, Hand R, Polleux F, and Ehlers MD (2010). TGF-beta signaling specifies axons during brain development. Cell 142, 144–157. [PubMed: 20603020]

Yin X, Takei Y, Kido MA, and Hirokawa N (2011). Molecular motor KIF17 is fundamental for memory and learning via differential support of synaptic NR2A/2B levels. Neuron 70, 310–325. [PubMed: 21521616]

Yoshimura T, Kawano Y, Arimura N, Kawabata S, Kikuchi A, and Kaibuchi K (2005). GSK-3beta regulates phosphorylation of CRMP-2 and neuronal polarity. Cell 120, 137–149. [PubMed: 15652488]

Zipursky SL, and Grueber WB (2013). The molecular basis of self-avoidance. Annu. Rev. Neurosci 36, 547–568. [PubMed: 23841842]

Zoghbi HY (2003). Postnatal neurodevelopmental disorders: meeting at the synapse? Science 302, 826–830. [PubMed: 14593168]

Highlights

- A cGMP-synthesis complex assembles on the Scribble scaffold and localizes to dendrites
- The Scribble-sGC association is necessary for apical dendrite development
- Kinesin motor KifC2 mediates Scribble localization to dendrites
- Localized cGMP might mediate dendrite development independently of axon formation

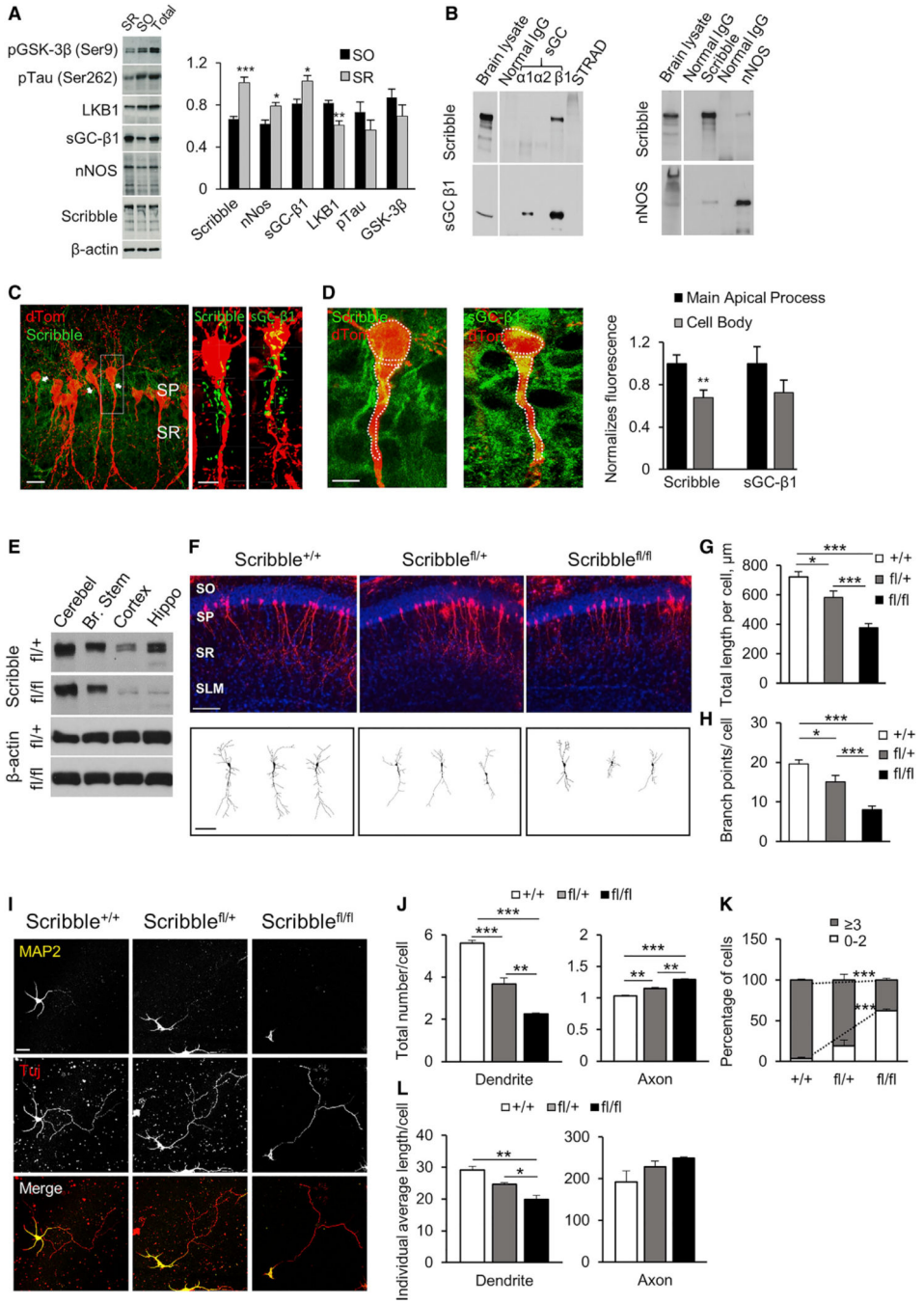

Figure 1. Scribble Scaffold Associates with and Is Necessary for Apical Dendrite Development in Embryonic CA1 Pyramidal Neurons

(A) Immunoblots of E20 rat embryonic lysates from stratum oriens (SO) versus stratum radiatum (SR; where CA1 apical dendrites are located) of CA1 region of the hippocampus and total brain lysates, with antibodies (Abs) to neuronal polarization proteins (pGSK-Ser9, pTau-Ser262, and LKB1), cGMP-synthesis enzymes sGC-β1 and nNOS, and Scribble. Right, expression quantified relative to that in total lysates (n = 5; Student's t test, *p < 0.05; **p ≤ 0.01; ***p ≤ 0.001).

(B) Co-Immunoprecipitation (Co-IP) of Scribble with sGC-β1 or nNOS from E18 brain lysates. Abs used for IP were sGC-β1, -α1, or -α2 subunits; Scribble; nNOS; or control protein STRAD. Immunoblotting (IB) with Scribble, sGC-β1, or nNOS. Normal immunoglobulin G (IgG), control for IP. Brain lysate, total brain lysate (n = 4).

(C and D) Localization of Scribble and sGC to CA1 apical dendrites. (C) Images of Scribble and sGC-β1 immunolabeling (green) in representative CA1 pyramidal neurons, at P7, following labeling with dTomato at E17.5. SP, stratum pyramidale. Scale bar represents 20 μm. Right, higher magnification images (boxed region, left). Scale bar represents 10 μm. (see also Figure S1). (D) Quantification of normalized Scribble or sGC-β1 immunofluorescence in apical dendrite versus soma (dashed lines) in CA1 pyramidal neurons. Right, average fluorescence intensity (Scribble and sGC-β1) in apical dendrite versus soma, normalized to that of dTom, presented as fold change relative to normalized apical dendrite signal (n = 12–15 cells; Student's t test, $^{**}p \leq 0.01$).

(E) Immunoblots of P0 $Scribble^{fl/fl}$ mouse brain lysates from cerebellum (Cerebel), brain stem (Br. Stem), cortex (Cortex), or hippocampus (Hippo), from heterozygous ($Scribble^{+/fl}$) or homozygous ($Scribble^{fl/fl}$) mouse littermates, with null Scribble allele generated using $Emx1^{Cre}$. IB with Scribble or β-actin (n = 3). Residual Scribble expression in homozygous $Emx1^{Cre/+}$;$Scribble^{fl/fl}$ cortex and hippocampus likely reflects expression in non-pyramidal neurons or non-neuronal cells.

(F) Representative images of P7 CA1 pyramidal neurons, from $Scribble^{+/+}$, $Scribble^{+/fl}$, or $Scribble^{fl/fl}$ littermates, transfected *in utero* at E15.5 with dTom. SLM, stratum lacunosum moleculare. Scale bar represents 50 μm. Bottom, sample tracings of 2D projection of neuritic arbor of representative neurons. Scale bar represents 20 μm.

(G) Quantification of average total apical dendrite length per cell, for CA1 pyramidal neurons from $Scribble^{+/+}$, $Scribble^{+/fl}$, or $Scribble^{fl/fl}$ littermates (n = 30 cells; one-way ANOVA, Tukey's post hoc, $^{*}p < 0.05$; $^{***}p \leq 0.001$).

(H) Quantification of average total apical dendrite branch points per cell, same dataset as in (G) (one-way ANOVA, Tukey's post hoc, $^{*}p < 0.05$; $^{***}p \leq 0.001$). (I) Images of representative cultured hippocampal neurons from $Scribble^{+/+}$, $Scribble^{+/fl}$, or $Scribble^{fl/fl}$ littermates, at 5 DIV, co-immunostained with MAP2 and Tuj-1. Scale bar represents 20 μm.

(J) Quantification of average axon and dendrite number per cell, at 5 DIV, in cultured hippocampal neurons from $Scribble^{+/+}$, $Scribble^{+/fl}$, or $Scribble^{fl/fl}$ littermates, based on MAP2 labeling (n = 3–5 cultures, 50–75 cells each; one-way ANOVA, Tukey's multiple comparison test; $^{**}p \leq 0.01$; $^{***}p \leq 0.001$).

(K) Quantification of average percentage of cells with only 0–2 dendrites or more than 3 dendrites, at 5 DIV; same dataset as in (J) (one-way ANOVA, Tukey'smultiple comparison test, $^{***}p \leq 0.001$).

(L) Quantification of average individual dendrite or axon length per cell; same dataset as in (J), at 5 DIV (one-way ANOVA, Tukey's multiple comparison test, $^{*}p \leq 0.05$; $^{**}p \leq 0.01$). $^{*}p < 0.05$, $^{**}p \leq 0.01$, $^{***}p \leq 0.001$. Error bars represent SEM.

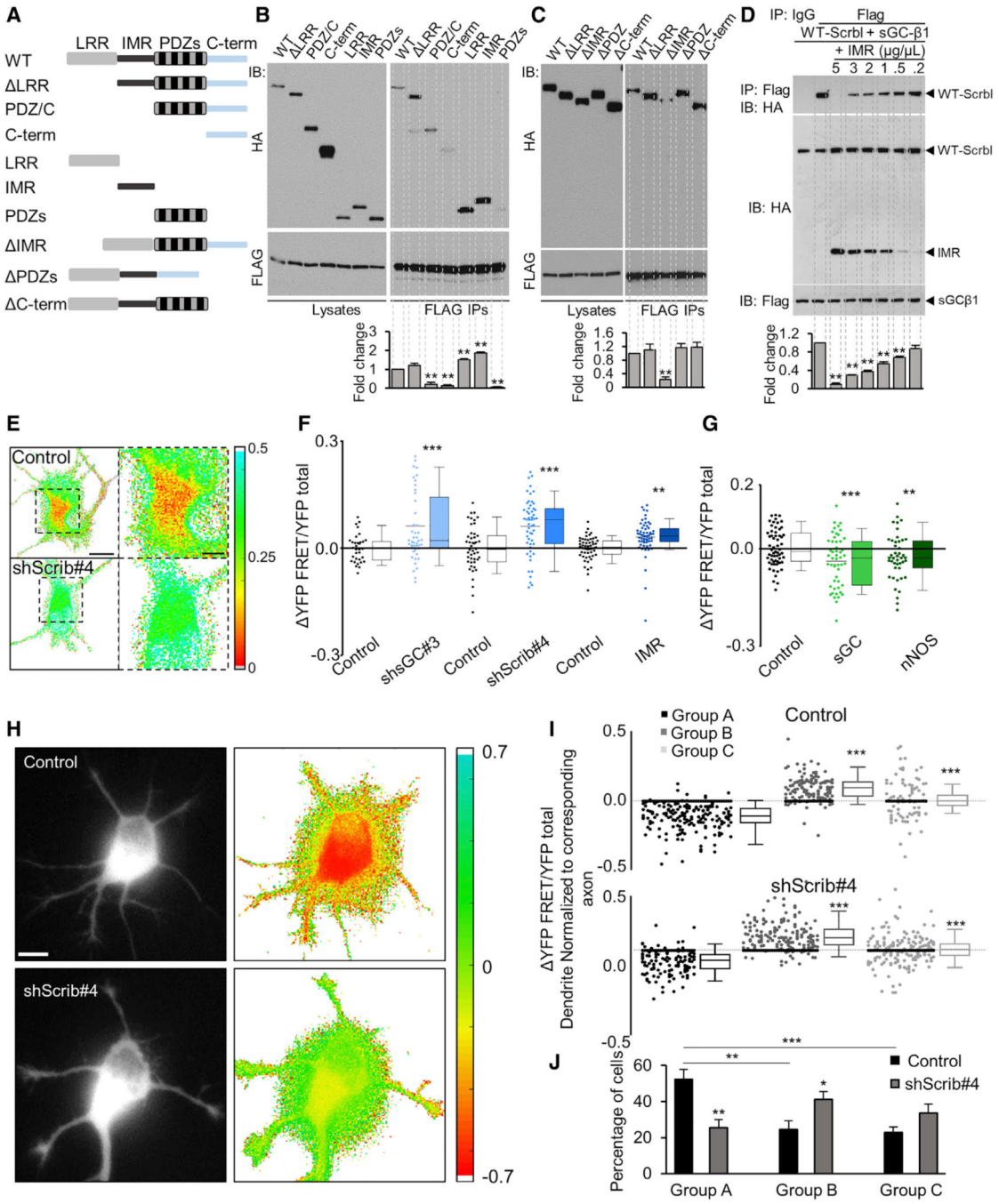

Figure 2. Scribble Forms a Complex for cGMP Increase in Dendrites

(A) Schematic depiction of the full-length (WT) Scribble protein and generated deletion mutants.

(B and C) coIP of Scribble, WT, or mutants, with sGC-b1, from HEK293 lysates co-expressing HA-fused Scribble proteins (A) and FLAG-fused sGC-β1. IP with FLAG (right panels) and IB with HA or FLAG. Lysates, total cell-lysates (left panels). IP quantified as fold change relative to WT-Scribble, normalized to total levels of the respective proteins (n = 4; one-way ANOVA; post hoc Dunnett's multiple comparison test, **p ≤ 0.01).

(D) coIP of full-length Scribble with sGC-β1, from HEK293 lysates co-expressing HA-Scribble and FLAG-sGC-β1, in the presence of increasing concentrations (0, 0.2, 0.5, 1, 2, 3, and 5 μg/μl) of HA-fused IMR domain, to tecst for Scribble-sGC-β1 complex disruption in the presence of IMR. Data quantified as fold change relative to control cells not expressing IMR (n = 3; one-way ANOVA; post hoc Dunnett's multiple comparison test, **p ≤ 0.01).

(E) Representative images of normalized somatic FRET signals for control- or Scribble-shRNA (ShScrib#4)-transfected cells. Normalized somatic FRET (YFP-FRET/YFP total) coded in pseudo-colors, for control or ShScrib#4-transfected cells co-expressing cGi-500. Scale bar represents 10 μm. Right, higher magnification images (of boxed regions on the left). Scale bar represents 5 μm. See also Figure S2B.

(F and G) Summary of difference in somatic FRET (ΔYFP-FRET/YFP total) relative to respective control for cells transfected with sGC-β1-shRNA, ShScrib#4, or IMR (F); or functional sGC enzyme or nNOS (G). Higher somatic FRET reflects somatic cGMP decrease and vice versa (n = 3–5 cultures, 20–30 cells each; F, Student's t test, **p ≤ 0.01, ***p ≤ 0.001; G, one-way ANOVA, Dunnett's multiple comparison test, **p ≤ 0.01, ***p ≤ 0.001).

(H) Representative images of normalized FRET signals in dendrites of control or ShScrib#4-transfected neurons. Difference between normalized FRET signals (ΔYFP-FRET/YFP total) of each dendrite of the neuron compared to that of the axon of the same cell, coded in pseudo-colors. Scale bar represents 10 μm. Left, original YFP total fluorescence images. FRET increase reflects cGMP decrease upon Scribble knockdown.

(I and J) Quantification of the difference in normalized FRET signals (ΔYFP-FRET/YFP total) between each dendrite of individual neurons (3 to 4 DIV) relative to that of the axon of that same neuron (signals averaged over the entire dendritic length and ~50-μm axonal segment), for all control or ShScrib#4 cells (see also Figure S2C). Neurons were categorized into three groups: A, most or all dendrites had lower normalized FRET (higher cGMP) than the axon; B, most or all dendrites had higher normalized FRET (lower cGMP) than the axon; and C, equal number of dendrites had higher or lower normalized FRET than the axon (n = 7 cultures; control, 78 cells; ShScrib#4, 88 cells) (I) One-way ANOVA, Dunnett's multiple comparison test, ***p ≤ 0.001. (J) Quantification of average percentage of cells in each group, in control or ShScrib#4 cells (one-way ANOVA, Dunnett's multiple comparison test, *p < 0.05, **p ≤ 0.01).

*p < 0.05, **p ≤ 0.01, ***p ≤ 0.001. Error bars represent SEM.

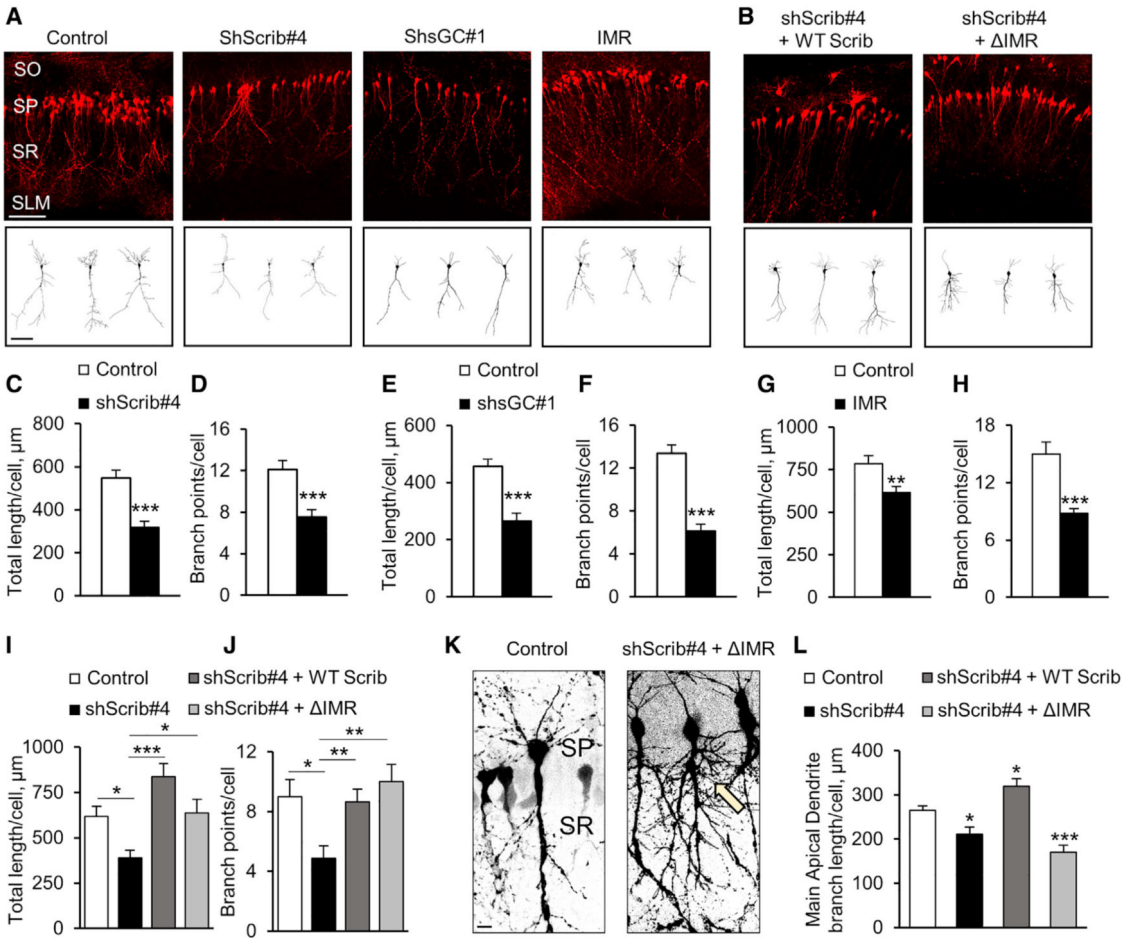

Figure 3. The cGMP-Production Complex Is Necessary for Apical Dendrite Development in the Embryonic CA1

(A and B) Representative images of P7 rat CA1 hippocampal pyramidal neurons, co-transfected *in utero* at E17.5 with dTom marker, together with either control-shRNA, ShScrib#4 or ShsGC#1 (effective Scribble or sGC-β1 knockdown, respectively), or IMR (A). ShScrib#4 was co-transfected with human (resistant to rat Scribble-shRNAs) WT Scribble or Scribble-ΔIMR (B). Control, control vector. Scale bar represents 100 mm. Bottom, sample tracings of 2D projection of neuritic arbor of representative neurons. Scale bar represents 20 µm.

(C, E, G, and I) Quantification of average total apical dendrite length per cell, for CA1 pyramidal neurons transfected with ShScrib#4 (C), ShsGC#1 (E), IMR (G), or co-transfected with ShScrib#4 with human WT- or ΔIMR-Scribble (I), compared to the respective control (n = 3–75 cells; C, E, G, Student's t test, $^{**}p \leq 0.01$, $^{***}p \leq 0.001$; I, one-way ANOVA, post hoc Newman-Keuls, $^{*}p < 0.05$; $^{***}p \leq 0.001$). For co-transfection of DIMR with ShScrib#4, see (K) and (L).

(D, F, H, and J) Quantification of total apical dendrite branch points per cell, for CA1 neurons, same dataset as in (C), (E), (G), and (I). (D, F, and H) Student's t test, $^{***}p \leq 0.001$; (J) one-way ANOVA, post hoc Newman-Keuls, $^{*}p < 0.05$, $^{**}p \leq 0.01$).

(K) Representative higher magnification images of P7 CA1 pyramidal neurons co-transfected with ShScrib#4 and human Scribble-ΔIMR. Scale bar represents 10 µm. Arrow

indicates shorter primary apical dendrite process exhibiting excessive and morphologically abnormal lateral branching.

(L) Quantification of average length of the primary branch of the apical dendrite per cell, for CA1 pyramidal neurons transfected with ShScrib#4, alone or togetherwith human WT- or ΔIMR-Scribble, compared to control (n = 20–50 cells; one-way ANOVA; post hoc Dunnett's multiple comparison test, *$p < 0.05$, **$p \leq 0.01$).

*$p < 0.05$, **$p \leq 0.01$, ***$p \leq 0.001$. Error bars represent SEM.

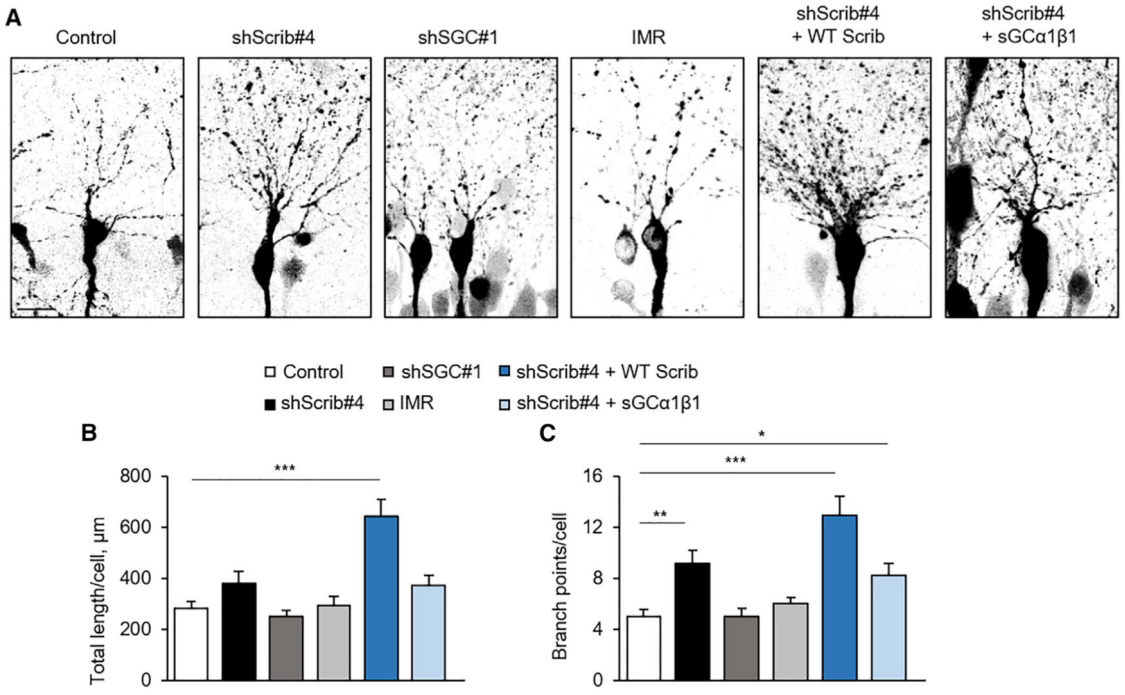

Figure 4. The cGMP-Production Complex Is Not Required for CA1 Basal Dendrite Development

(A) Representative high-magnification images of basal dendrites of individual P7 rat CA1 pyramidal neurons, co-transfected *in utero* with either control-shRNA, ShScrib#4 or ShsGC#1, or IMR, together with dTom marker. To test for rescue following Scribble knockdown, ShScrib#4 was co-transfected with human WT Scribble or functional sGC (rat sGC-α1 and -β1 subunits). Scale represents 20 μm.

(B and C) Quantification of average total basal dendrite length (B) or branch points (C) per cell, for CA1 pyramidal neurons transfected with ShScrib#4 or ShsGC#1, IMR, or co-transfected with ShScrib#4 with human WT-Scribble or sGC, compared to control (n = 20–90 cells; one-way ANOVA, Dunnett's multiple comparison test, *$p < 0.05$, **$p \leq 0.01$, ***$p \leq 0.001$).

*$p < 0.05$, **$p \leq 0.01$, ***$p \leq 0.001$. Error bars represent SEM.

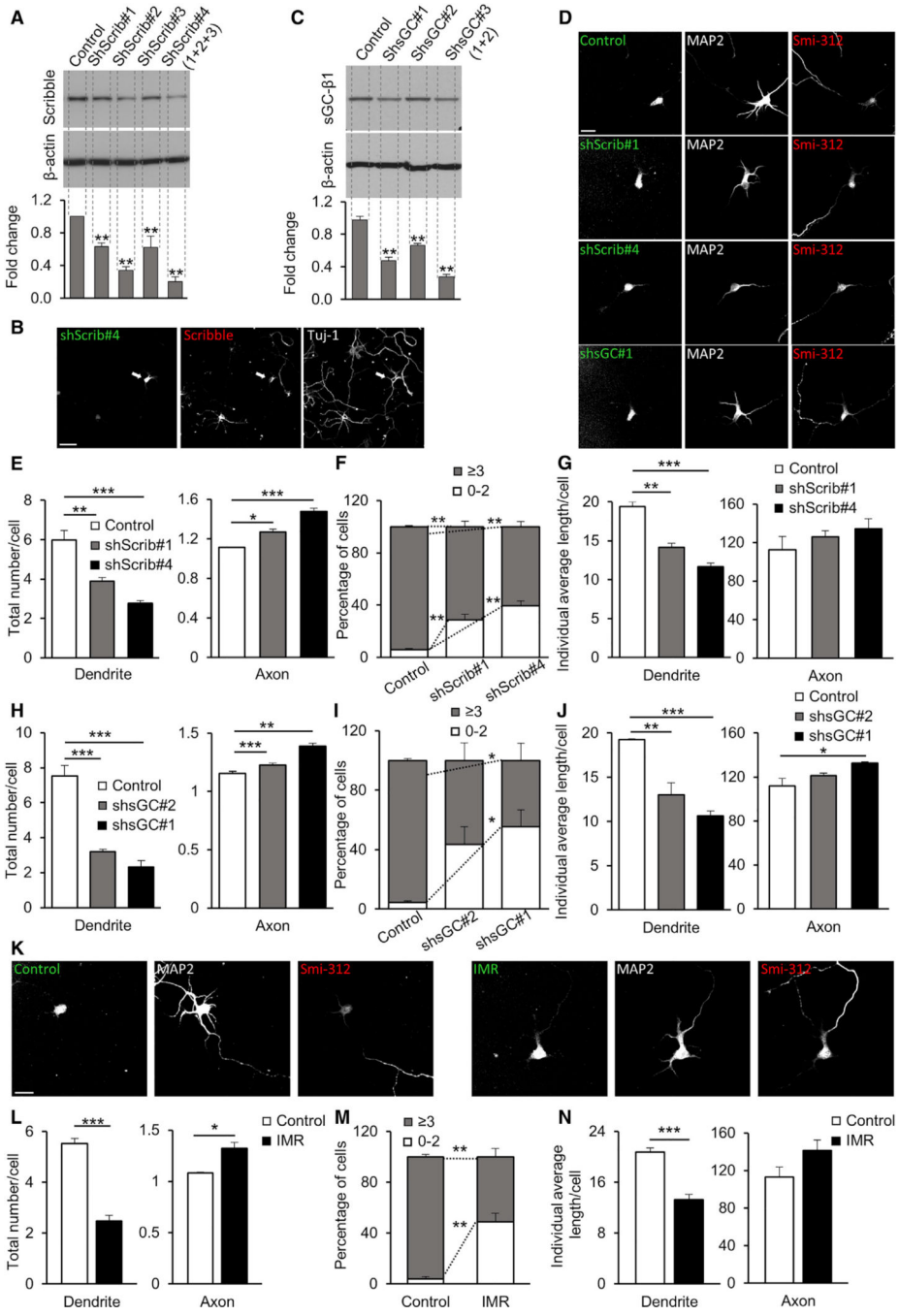

Figure 5. The cGMP-Production Complex Is Necessary for Dendrite Formation in Cultured Hippocampal Neurons

(A and C) Knockdown of Scribble (A) or sGC-β1 (C) in HEK293 cells with shRNAs targeting rat Scribble (ShScrib#1, #2 or #3; ShScrib#4, combined pool ShScrib#1 + #2 + #3) (A) or rat sGC-b1 (ShsGC#1 and #2; ShsGC#3, pool of ShsGC#1 + #2) (C), co-transfected in HEK293 cells together with targeted HA-Scribble (A) or sGC-β1 (C). Control, control shRNA. Scribble (A) or sGC-β1 (C) levels quantified as fold reduction (n = 3; one-way ANOVA; post hoc Dunnett's multiple comparison test, $^{**}p \leq 0.01$) relative to control shRNA.

(B) Images of representative polarized hippocampal neurons (5 DIV) transfected with ShScrib#4 (arrowhead), next to non-transfected cell, immunostained for Scribble and Tuj-1. Scale bar represents 40 μm.

(D and K) Representative images of hippocampal neurons (5 DIV) transfected with ShScrib#1 or ShScrib#4 (D), which showed moderate or strong efficiency in Scribble knockdown, respectively (A), or ShsGC#1 (D) that showed strong efficiency in sGC-b1 knockdown (C), control-shRNA (D), or EGFP-fused IMR domain or control vector (K). Neurons are co-labeled with MAP2 and Smi-312. Scale bars represent 40 mm.

(E, H, and L) Quantification of average axon and dendrite number per cell (5 DIV), based on immunostaining with MAP2 and Smi-312, for cells transfected with Scribble- (E) or sGC-β1-shRNAs (H), IMR domain (L), or control vectors (n = 3–5 cultures, 50–75 cells each; E and H, one-way ANOVA, Tukey's multiple comparison test, *$p < 0.05$, **$p \leq 0.01$, ***$p \leq 0.001$; L, Student's t test, *$p < 0.05$, ***$p \leq 0.001$).

(F, I, and M) Quantification of the average percentage of cells with 0–2 dendrites or more than 3 dendrites (5 DIV), based on immunostaining with MAP2 and Smi-312, for cells transfected with Scribble- (F), sGC-β1-shRNAs (I), IMR (M), or control vectors; same dataset as in (E), (H), and (L) (F, I, one-way ANOVA, Tukey's multiple comparison test, p* < 0.05, p** ≤ 0.01; M, Student's t test, **$p \leq 0.01$).

(G, J, and N) Quantification of average individual dendrite or axon length per cell; same dataset as in (E), (H), and (L); 5 DIV. (G and J, one-way ANOVA, Tukey's multiple comparison test, *$p < 0.05$, **$p \leq 0.01$, ***$p \leq 0.001$; N, Student's t test, ***$p \leq 0.001$). *$p < 0.05$, **p % 0.01, ***p % 0.001. Error bars represent SEM.

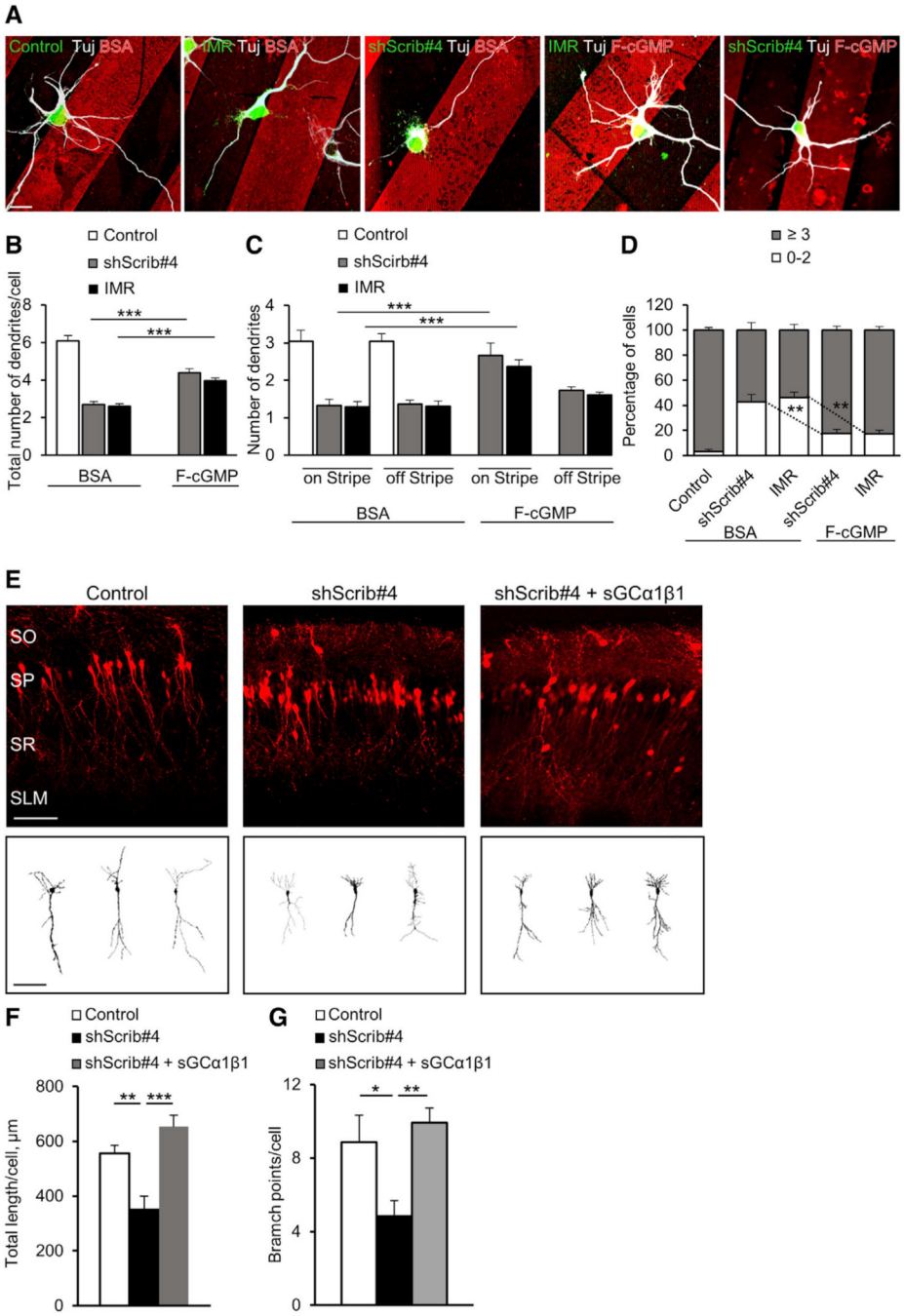

Figure 6. Local cGMP Elevation or sGC Expression Rescued Dendrite Defects following Scribble Knockdown

(A) Representative images of hippocampal neurons, transfected with ShScrib#4 or control-shRNA, or EGFP-fused IMR or control vector, plated on substrates coated with stripes of membranepermeable fluorescent analog of cGMP (F-cGMP, red) or control fluorescently conjugated BSA (5 DIV) immunostained with Tuj-1. Shown are neurons with their soma located at the stripe boundary. Scale bar represents 20 μm.

(B and C) Quantification of average total dendrite number per cell (B) or dendrite number initiated in the “on-stripe” or “off-stripe” region of F-cGMP or BSA stripe (C), for polarized

neurons with their soma located at the stripe boundary (5 DIV) for cells transfected with ShScrib#4 or control-shRNA, or IMR or control vector (n = 3–5 cultures, 50–75 cells each; one-way ANOVA, Tukey's multiple comparison test; ***p ≤ 0.001).

(D) Quantification of the average percentage of cells with 0–2 or more than 3 dendrites (5 DIV) for the same dataset as in (B) and (C) (one-way ANOVA, Tukey's multiple comparison test, **p ≤ 0.01).

(E) Representative images of P7 rat CA1 pyramidal neurons, transfected *in utero* with control-shRNA, or ShScrib#4 alone or together with functional sGC enzyme (rat sGC-α1 and -β1 subunits), to test for rescue of Scribble knockdown with sGC. Scale bar represents 100 mm. Bottom, sample tracings of neuritic arbor of representative neurons. Scale bar represents 20 μm.

(F and G) Quantification of average total apical dendrite length (F) or branch points (G) per cell, for CA1 pyramidal neurons transfected with control-shRNA or ShScrib#4 alone or with reconstructed sGC (n = 20–30 cells; one-way ANOVA, Tukey's multiple comparison test, *p < 0.05, **p ≤ 0.01, ***p ≤ 0.001).

*p < 0.05, **p ≤ 0.01, ***p ≤ 0.001. Error bars represent SEM.

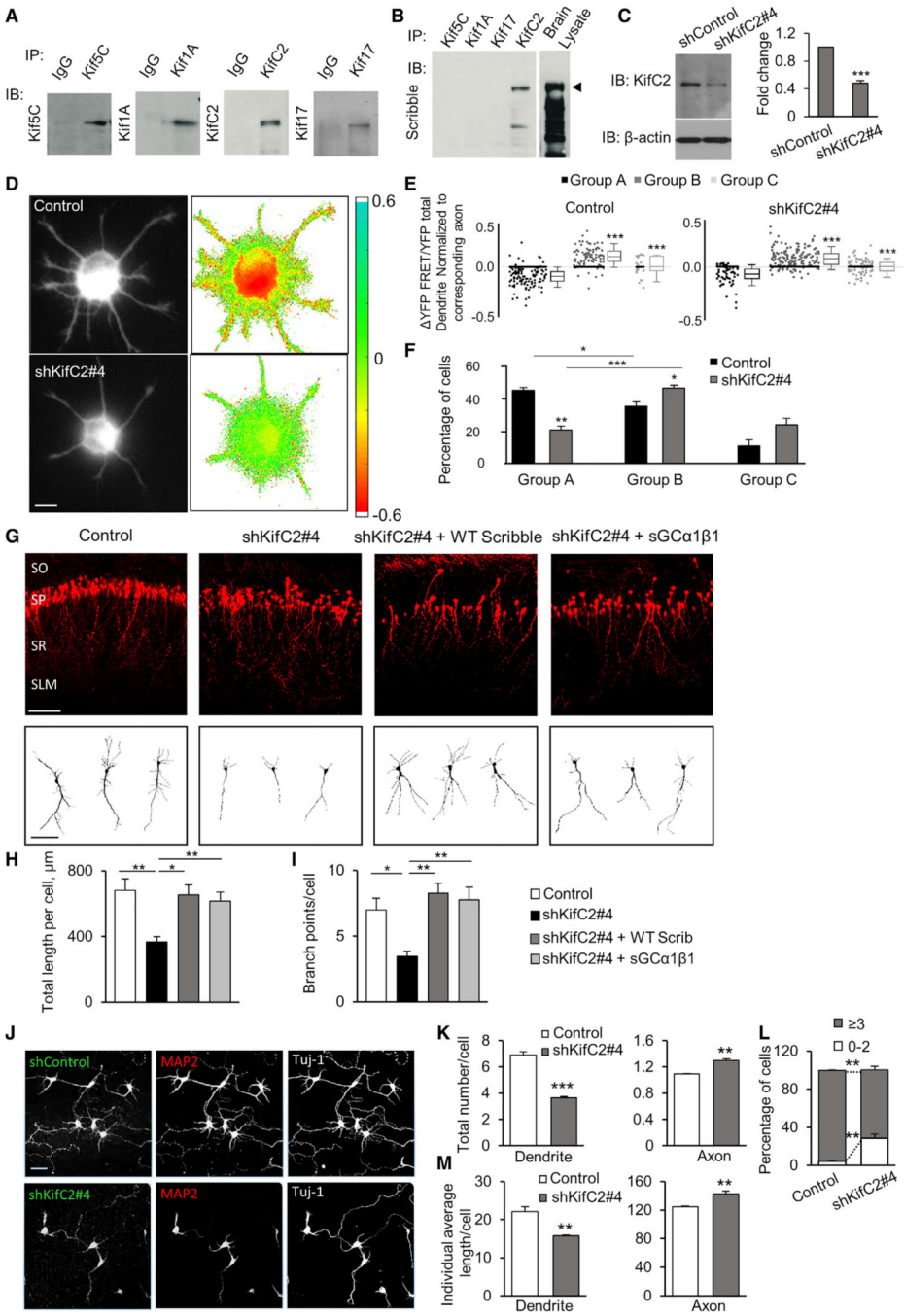

Figure 7. Scribble and Kinesin KifC2 Association Is Necessary for Dendritic cGMP Regulation and Apical Dendrite Development

(A) IP and IB of E18 rat embryonic brain lysates with Abs to Kif5C, Kif1A, KifC2, or Kif17. Control, IP with non-specific IgG (IgG). (n = 3).

(B) coIP of Scribble with kinesins from the embryonic brain. IP from E18 brain lysates with Kif5C, Kif1A, KifC2, or Kif17. IB, Scribble. Brain lysate, total brain lysate. (n = 3).

(C) Knockdown of KifC2 in cultured hippocampal neurons. ShKifC2#4 (combined pool of ShKifC2#1 + #2 + #3) transfected in cultured hippocampal neurons and whole-cell extracts

immunoblotted for KifC2 (3 DIV). shControl, control shRNA. KifC2 levels quantified as fold reduction relative to control shRNA (n = 4; Student's t test, ***p ≤ 0.001).

(D) Representative images of normalized FRET signals in dendrites of control- or ShKifC2#4-transfected neurons. Difference in normalized FRET signals (ΔYFP-FRET/YFP total) between the axon and dendrites are coded in pseudo-colors (as in Figure 2H). Scale bar represents 10 μm. Left, YFP total fluorescence images.

(E and F) Quantification of the difference in normalized FRET (ΔYFP-FRET/YFP total) between the axon and dendrites of individual neurons (3 to 4 DIV), for all control or ShKifC2#4 cells. Neurons categorized into three groups, namely, A, B, and C (as in Figures 2I and 2J) (E, one-way ANOVA, Dunnett's multiple comparison test, **p ≤ 0.01). (F) Quantification of average percentage of cells in each group in control or ShKifC2#4 cells (n = 3 cultures; Control, 53 cells; ShKifC2#4, 62 cells; one-way ANOVA, Dunnett's Multiple Comparison Test, *p < 0.05, **p ≤ 0.01).

(G) Representative images of P7 rat CA1 pyramidal neurons, transfected *in utero* with control-shRNA, or ShKifC2#4 alone or together with WT human Scribble or functional sGC enzyme. Scale bar represents 100 mm. Bottom, sample tracings of a 2D projection of neuritic arbor of representative neurons. Scale bar represents 20 μm.

(H and I) Quantification of average total apical dendrite length (H) or branch points (I) per cell, for CA1 pyramidal neurons transfected with control-shRNA or ShKifC2#4, alone or with WT human Scribble or reconstructed sGC (n = 20–30 cells; one-way ANOVA, Tukey's multiple comparison test, *p < 0.05, **p ≤ 0.01).

(J) Representative images of hippocampal neurons (5 DIV) transfected with ShKifC2#4 or control-shRNA, co-immunostained with MAP2 and Tuj-1. Scale bar represents 40 μm.

(K) Quantification of average axon and dendrite number per cell (5 DIV), based on immunostaining with MAP2 and Smi-312, for cells transfected with ShKifC2#4 orcontrol-shRNA (n = 3–4 cultures, 50–75 cells each; Student's t test, **p ≤ 0.01, ***p ≤ 0.001).

(L) Quantification of the average percentage of cells with 0–2 or more than 3 dendrites (5 DIV), based on MAP2 and Smi-312 labeling, for ShKifC2#4 or control-shRNA cells; same dataset as in (K) (Student's t test, **p ≤ 0.01).

(M) Quantification of average individual dendrite or axon length per cell; same dataset as in (K); 5 DIV (Student's t test, **p ≤ 0.01).

*p < 0.05, **p ≤ 0.01, ***p ≤ 0.001. Error bars represent SEM.

KEY RESOURCES TABLE

REAGENT or RESOURCE	SOURCE	IDENTIFIER
Antibodies		
rabbit anti Scribble (H-300)	Santa Cruz	Cat# sc-28737; RRID:AB_2184807
rabbit anti nNOS (R-20)	Santa Cruz	Cat# sc-648; RRID:AB_630935
mouse anti-HA	Santa Cruz	Cat# sc-7392; RRID:AB_627809
rabbit anti β-actin	Cell Signaling Technology	Cat# 4967; RRID:AB_330288
rabbit anti sGC-β1	Cayman chemical	Cat# 160897; RRID:AB_10080042
rabbit anti KifC2 [N3C2]	GeneTex	Cat# GTX124082; RRID:AB_11167943
rabbit anti KifC2	Thermo Fisher Scientific	Cat# PA5-56098, RRID:AB_2643118
mouse anti-FLAG®M2	Sigma-Aldrich	Cat# F1804; RRID:AB_262044
rabbit anti Tuj1	Covance	Cat# PRB-435P-100; RRID:AB_291637
chicken anti MAP2	Novus Biologicals	Cat# NB300-213; RRID:AB_2138178
mouse anti-GFP	Roche	Cat# 11814460001; RRID:AB_390913
Alexa Fluor® 488 AffiniPure Goat Anti-Mouse IgG	Jackson ImmunoResearch	RRID: AB_2338840
Alexa Fluor® 594 AffiniPure Goat Anti-Mouse IgG	Jackson ImmunoResearch	RRID: AB_2338871
Alexa Fluor® 594 AffiniPure Goat Anti-Rabbit IgG	Jackson ImmunoResearch	RRID: AB_2338059
Alexa Fluor® 488 AffiniPure Goat Anti-Rabbit IgG	Jackson ImmunoResearch	RRID: AB_2338046
Alexa Fluor® 647 AffiniPure Goat Anti-Rabbit IgG	Jackson ImmunoResearch	RRID: AB_2338072
Alexa Fluor® 594 AffiniPure Goat Anti-Chicken	Jackson ImmunoResearch	RRID: AB_2337391
rabbit anti STRAD (Y-25)	Santa Cruz	Cat# sc-130882; RRID:AB_2197574
Bacterial and Virus Strains		
DH5α competent cells	Life Technologies	Cat#18265017
Chemicals, Peptides, and Recombinant Proteins		
Fluorescently conjugated Bovine Serum Albumin (BSA)	Life Technologies	Cat#A13100

REAGENT or RESOURCE	SOURCE	IDENTIFIER
Guanosine- 3′, 5′- cyclic monophosphate, acetoxymethyl ester (cGMP-AM)	BIOLOG	Cat#G002
Hoescht 33342 (bis-benzimide 33342)	Sigma-Aldrich	Cat#B2261
Triton X-100	Millipore Sigma	Cat#TX1568-1
Fast Green	Sigma-Aldrich	Cat#F7252
Fluoromount-G	SouthernBiotech	Cat#0100-01
Phosphate buffered saline	Sigma-Aldrich	Cat#P4417
Normal Goat Serum	Jackson ImmunoResearch	RRID: AB_2336990
Amersham Hyperfilm ECL	GE Healthcare	Cat#28906839
Amersham ECL Western Blotting Detection Reagents	GE Healthcare	Cat#RPN2209
Protein G agarose	Roche	Cat#11719416001
CHAPS hydrate	Millipore Sigma	Cat#9426
Nitrocellulose Membranes 0.45um	BIO RAD	Cat#1620115
Tween 20	BIO RAD	Cat#170-6531
Paraformaldehyde	Milipore Sigma	Cat#441244
0.25% Trypsin-EDTA	GIBCO	Cat#25200056
GlutaMAX	GIBCO	Cat#35050061
Neurobasal Medium minus Phenol Red	GIBCO	Cat#12348017
Neurobasal Medium	GIBCO	Cat#21103049
Hibernate E minus CaCl2	BrainBits	Cat#HECA
Hibernate E	BrainBits	Cat#HE
Papain	Worthington Biochemical Corporation	Cat#LK003178
Poly-L-Lysine Hydrochloride	Millipore Sigma	Cat#P9404
B-27 Supplement	Life Technologies	Cat#17504044
Critical Commercial Assays		
EndoFree Plasmid Maxi Kit	QIAGEN	Cat#12362
Experimental Models: Cell Lines		

REAGENT or RESOURCE	SOURCE	IDENTIFIER
HEK293	ATCC	Cat# PTA-4488
Experimental Models: Organisms/Strains		
CD® (Sprague Dawley) rats	Charles River	RRID:RGD_734476
B6.129S2-Emx1tm1(cre)Krj/J mice	Jackson Laboratory	RRID:IMSR_JAX:005628
Conditional Scribble$^{flox/flox}$ mice	Gift from Dr. T.B. Huber, Department of Medicine, University Medical Center Hamburg-Eppendorf, Hamburg,	N/A
Oligonucleotides		
shScrib#1	This study	GATCCCAGAGATCTTGAAGTGCTTCTTTTGATATCCGAAGAAGCACTTCAAGATCTCTTTTTTTCCAAA
shScrib#2	This study	GATCCCAGGGAGAGATTTAAGCAGGTTTTGATATCCGAACCTGCTTAAATCTCTCCCTTTTTTTCCAAA
shScrib#3	This study	GATCCCGCCCTGTAGTCAAACTTCTTTTTGATATCCGAAAGAAGTTTGACTACAGGGCTTTTTTCCAAA
shKifC2#1	This study	GATCCCGAAGTCTACTCAGCTCTTCTTTTGATATCCGAAGAAGAGCTGAGTAGACTTCTTTTTTCCAAA
shKifC2#2	This study	GATCCCGCAAGAGCTGACTTGTTACTGTTTGATATCCGACAGTAACAAGTCAGCTCTTGTTTTTTCCAAA
shKifC2#3	This study	GATCCCGTGTCAGTACTGAGAGAAGAATTGATATCCGTTCTTCTCTCAGTACTGACACTTTTTTCCAAA
Recombinant DNA		
PRNT U6.1 vector	GeneScript	N/A
shScrib#1	This study	N/A
shScrib#2	This study	N/A
shScrib#3	This study	N/A
pCAGJC-HA-rat Scribble, Scribble-cDNA	This study	N/A
DLRR	This study	N/A
PDZ/C	This study	N/A
C-term	This study	N/A
LRR	This study	N/A
IMR	This study	N/A
PDZs	This study	N/A
DIMR	This study	N/A
DPDZs	This study	N/A
DC-term	This study	N/A
pCAGJC-FLAG-nNOS	This study	N/A
pcDNA3.1 nNOS-GFP	Gift from Dr. Bonnie Firestein, Rutgers, the	N/A

REAGENT or RESOURCE	SOURCE	IDENTIFIER
	State University of New Jersey, Piscataway, NJ	
pCAGJC-FLAG-rat sGC-β1	This study	N/A
pCAGJC-dTomato	Shelly et al., 2007	N/A
pCAGJC-EGFP	Shelly et al., 2007	N/A
shKifC2#1	This study	N/A
shKifC2#2	This study	N/A
shKifC2#3	This study	N/A
Software and Algorithms		
ImageJ Fiji software		RRID:SCR_002285
Prism v8.1.2	GraphPad	RRID:SCR_002798
IMRS 7.3.1	Bitplane	RRID:SCR_007370